Høgskolen i Østfold

MASTER THESIS

Design and Model Predictive Control of Transcritical CO_2 Heat Pumps for Residential Application

Mohammad Shakerin

15.08.2023

Master in Green Energy Technology
Faculty of Computer Science, Engineering and Economics

Abstract

Ground source TCCO2HP systems have garnered attention for their potential in enhancing energy efficiency in residential settings. Recognizing their significance, this study delves into the creation of a high-fidelity physical model of such a system tailored for a standard detached residential suite. The comprehensive heating system was meticulously broken down into subsystems, categorized by their energy carrier domain and specific functionality. To implement Model Predictive Control (MPC), a mathematical representation encapsulating the system's dynamic behaviour was derived. This representation was subsequently refined and integrated into the MPC framework as an internal state prediction model. To validate the effectiveness of the models, they were tested against a hypothetical residential scenario. This involved analysing the system's performance under diverse weather conditions and comparing it with conventional controllers. The findings were promising. The MPC not only outperformed in ensuring optimal thermal comfort but also steered the transcritical operation towards a consistently higher and more stable Coefficient of Performance (COP). This research underscores the potential of MPC in optimizing the performance of ground source TCCO2HP systems in residential applications.

Table of contents

List of figures

Introduction

Climate change and its potentially severe consequences has been a worldwide concern for the past few decades. Reduction of Greenhouse Gas (GHG) is nentral to all the mitigation strategies and action plans, especially carbon dioxide. Reducing CO2 is considered the most important global warming action primarily because it is the most abundant GHG emitted by human activities, accounting for roughly 75% of total GHG emissions [1]. Besides, reducing CO2 is vital for long term climate sustainability. Carbon dioxide has a long atmospheric lifetime, lasting between 50 to 200 years, which means that it continues to contribute to global warming for an extended period after it is emitted. In addition, CO2 is emitted from a wide range of human activities, including the burning of fossil fuels for electricity generation, transportation, and industrial processes [2]. In 2020, the global energy consumption of residential buildings was reported 22%, and the carbon dioxide (CO_2) emissions associated with them increased to the highest share of 17% [1, 3]. The majority of the energy usage in residential buildings in European Union (EU) is dedicated to heating services for domestic hot water (DHW) consumption and space heating (SH) [1]. With the expected population growth in the coming years, the energy demand for residential buildings will rise remarkably. Thus, taking rigorous actions to increase energy conversion efficiency both at component and system levels is vital [1, 3]. In this regard, EU has established several progressive directives and legislation, promote high energy efficiency and decarbonization in the building sector by 2050. In general, to achieve carbon neutrality in the building sector improvement actions are over three main axes, 1) clean and renewable energy generation, 2) energy conversion and distribution efficiency, 3) energy consumption reduction and management. However, the rate of integration of renewable energy sources (RES) in building thermal energy system has been ahead of technological improvements in energy conversion efficiency and reduction of energy demands [3].

In recent years, there has been a noticeable increase in research and development of building energy systems powered entirely by heat pumps. This surge is driven by policies and legislation focused on improving building energy efficiency and considering environmental impacts [4]. Heat pumps are proven to be sustainable solutions for supplying residential heating, using the abundant low-grade heat from surroundings (e.g. air, water, ground, etc.) as the heat source. Besides, heat pumps are able to facilitate the integration of other modern building energy technologies such as local renewable energy generation and thermal energy storage [5-7]. To date, the working principle of heat pump systems is well-established. However, the improvement potentials are still largely untapped, mainly due to the limited capacity, delivered temperature ranges, and environmental impacts of conventional systems working with synthetic refrigerants.

Carbon dioxide as a trending refrigerant

Over the last decades, heat pump solutions for modern residential buildings have matured. This progress is not just due to advancements in energy infrastructure, but also the development of synthetic refrigerants. These refrigerants offer reliable operation and manageable manufacturing complexity, allowing them to work with traditional control mechanisms. This has accelerated the commercialization of heat pumps. [8]. However, following the Montreal protocol on the protection of the ozone layer in 1987, synthetic refrigerants are actively being planned to be phased out and replaced by natural refrigerants worldwide [9-11]. This has triggered rigorous research and developments of heat pump system designs using natural refrigerants [12].

Among other refrigerants, CO_2 is a well-known refrigerant featuring zero ozone layer depletion potential and the lowest global warming potential. In addition, CO_2 has proven to be superior due to relatively higher efficiency and delivered temperatures when operating in trans-critical, while being nontoxic (unlike Ammonia) and non-flammable (unlike Ethane) [8, 13]. It is proven that the unique sensible heat dissipation process in the supercritical region of CO_2 can heat water to high temperatures [14, 15] [7]. Hence, a transcritical CO_2 heat pump ($TCCO_2HP$) technology might be a suitable option when a large temperature difference in the heat delivery side exists [7, 16, 17]. This could be the case with residential heating, as the thermal energy demand of buildings varies depending on the season, time of the day, and end-use purpose. Systems for hot water supply often experience high-temperature differences between supply and return, while space heating applications require less temperature gap in the circuit [7]. Given this compatibility, the potential for significant energy savings becomes evident, especially when viewed from a global user market perspective [12] [14].

Gap in design and controlling knowledge for CO_2HP.

In recent times, the home application of CO2 heat pumps has earned acclaim, both for its potential to enhance energy efficiency and better the quality of human life [12]. However, the widespread utilization of TCCO_2HP for households is still hampered by a lack of efficient design and control solutions that tackle the distinct operating challenges associated with the trans-critical CO_2 vapour compression cycle. Compared to conventional subcritical heat pumps, TCCO_2HP operates at higher pressure levels, necessitating a sophisticated compressor design and control [18]. Due to the sensitivity of optimal performance on multiple sizing and operational criteria, issues such as increased exergy loss at the gas cooler and expansion valve, and control design malfunctioning in realistic operation conditions are prevalent [2, 19]. For example, one of the most sensitive performance parameters is the heat exchanging process at the gas cooler with trans-critical CO_2 [16]. A high coefficient of performance (COP) for the TCCO_2HP demands an optimal tuning of the water temperature rise, as it determines the heat exchange efficiency at the gas cooler. This feature greatly distinguishes the robust design and control approaches for TCCO_2HP from the conventional sub-critical heat pumps [20]. Moreover, the coupling of TCCO_2HP with advanced sustainable energy solutions in the buildings and occupants' consumption patterns can aggravate the control and operational burden of TCCO_2HP.

Previous research has shown both merits and challenges of compression cycle of co2 near its critical point [16, 21-26]. Many studies attempted to characterize the heat pump performance in transtritical region, have found an optimality of states, in which the efficiency is maximized. Investigations on developing procedures for the optimal control of TCCO_2HP in relation to various energy dynamics in TCCO_2HP, shows multitude of factors such as compressor discharge pressure [27, 28], expansion valve position [27], water return temperature [23], and mass flow rates, having significant impacts on the optimal operation range [2]. Several experimental and numerical designs TCCO_2HP have been proposed with distinct enhancement features [29].

While there has been a noticeable upswing in research related to CO_2 heat pumps in recent years, with a particular focus on optimizing transcritical operations, the real-world application of such systems for residential contexts remains under-explored. A significant portion of these studies tend to revolve around design and performance correlations tailored specifically for air source systems. Conversely, the exploration into water-water CO_2 heat pumps has been limited, and ground-coupled solutions appear to be even more scant [30, 31]. The potential advantages of ground-coupled systems are noteworthy. The ground, due to its relatively consistent temperature throughout the year, offers a stable heat source. This stability can make heat extraction less strenuous and, in turn, alleviate the control demands of the vapor compression cycle. Given that the designing of an appropriate configuration and controlling the system around the optimal operating point present inherent challenges, integrating advancements in optimal control methods coupled with alternative sustainable solutions for building energy systems can offer significant benefits.

Model predictive control

Traditional control strategies, such as PID or on/off controllers, operate on a reactive basis. In these systems, a sensor first detects a disturbance signal, and then a corresponding control action is applied. These strategies are been used in many control systems due to their simplicity, reliability, and ease of implementation [32, 33]. On the other hand, Model Predictive Control (MPC) represents a more advanced and proactive approach to system control. Instead of merely reacting to disturbances, MPC anticipates future events by solving an optimization problem based on the current state or model of the system. This optimization aims to devise a control scheme that minimizes an objective function over a defined prediction horizon. While doing so, it takes into account system constraints, current control trajectories, and potential future disruptions [34, 35]. A key strength of MPC lies in its ability to incorporate the relationship between system inputs and outputs, their dynamics, and feedback loops into its prediction model. This comprehensive modelling is central to the MPC concept and allows for a more adaptive control strategy [32, 36]. Furthermore, system constraints can be directly integrated into the MPC, which not only streamlines the design process but also refines the objective function. This embedded consideration of constraints ensures that the system operates within safe and efficient parameters, reducing the risk of overshoots or system instability [34, 37].

Numerous studies on the development of predictive control concepts together with the advancement of data processing techniques during the past decade revealed both practical limitations and improvement potentials for building energy systems [34, 37-39]. Although some viable options for MPC solutions for single optimization applications are currently available, implementation of MPC in advanced building energy systems reported challenges such as high dependency on the quality of the future forecasts [34, 39]. Due to high computational complexity, most of the previous methods were proposed for a limited number of system states and often did not include most of the smart building features [40].

Regarding the optimal control of TCCO_2HP, MPC stands out primarily due to its inherent versatility and adaptability to changing conditions. This might turn TCCO_2HP well-suited for integration with modern building energy technologies, such as short- and long-term thermal energy storages, solar and wind power systems. Yet currently the integration of MPC and CO_2 heat pump operations remains an underrepresented area of study. As such, there lies a promising avenue for research, which can explore the potential synergies between MPC and CO_2 heat pumps, especially in residential settings.

One of the most challenging parts of the TCCO_2HP development for buildings heating systems is the identification of optimized design and control solutions with respect to the building energy dynamics, including the construction properties, HVAC and DHW systems, and other processes with a desirable balance between accuracy and computational burden. In this regard, often the model characteristics are defined in isolation which usually limits inherent prediction strength of the MPC structure. Alternatively, data-driven approaches for the systematic design of MPC are gaining attention because the complex human-system interactions as well as partial or unstable input-output relations can be treated more effectively [34, 37-39]. However, the effectiveness of these approaches is highly dependent of the available data about the behaviour of the system. The highly nonlinear characteristic of energy processes in buildings demands for holistic high-fidelity models or sophisticated data-driven models.

Objectives

This research aimed to address the current demand for efficient design and control of TCCO_2HPs for residential sector. In particular, the objective of this study is to perform an analysis on the potentials of MPC to improve operation of residential ground source TCCO_2HPs. In this regard, this study endeavours to:

1. Design and establish a dynamic model of a ground sourced TCCO_2HP system to meet residential hot water and space heating demands.

2. To implement an MPC approach for control of the building energy system.
3. To evaluate the performance of the MPC-controlled $TCCO_2HP$ in terms of energy conversion efficiency, Thermal comfort satisfaction.

Scope

This research focuses on the key components of a modern residential heating system, which includes the building's structure and the energy conversion processes driven by the heat pump cycle. While the study delves into the core heat transfer characteristics of TCCO2HP, it does not go into the intricate, case-specific designs of every equipment within the system. Essentially, the research provides a broad overview of TCCO2HP technology, aiming for the findings to be applicable across various contexts.

Outline

The structure of this thesis unfolds as follows: Chapter 2: Literature review, delves into the theoretical background, laying the foundation for the study. Chapter 3: Methods, elucidates the methods used for developing physical modelling of the residential TCCO2HP systems, as well as designing a suitable MPC controller for the system . The subsequent Chapter 4: Case study, presents a case study, offering a practical perspective into the presented method. Chapter 5: Results, showcases the results, which are then critically analysed in Chapter 6: Discussion. Finally, Chapter 7: Conclusion, concludes the thesis, summarizing the key findings and their implications.

2. Literature review

To comprehend the dynamics and characteristics of CO_2 heat pumps, especially when applied to residential heating, it's crucial to delve into the fundamental theories and historical developments. This chapter explores the fundamental principles of CO_2 as a refrigerant, its role in heat pumps, and the transformative impact of MPC in ensuring optimal operations. Furthermore, the chapter will highlight the potential of MPC in enhancing the performance of $TCCO_2HP$ for domestic thermal energy supply. By drawing from previous findings, this chapter lays the groundwork necessary to model and control a ground sourced $TCCO_2HP$ for residential heating.

Distinct characteristics of carbon dioxide

utilizing CO_2 as a working medium introduces specific challenges and advantages due to its unique thermodynamic properties. Upon reaching a critical temperature of 31.1 °C and a critical pressure of 73.7 bar, CO_2 transitions into its supercritical phase. Close to critical point, CO_2 displays erratic thermodynamic characteristics similar to both gas and liquid phase. As shown in Figure 1 and Figure 2, its density and thermal conductivity varies significantly [41] [42].

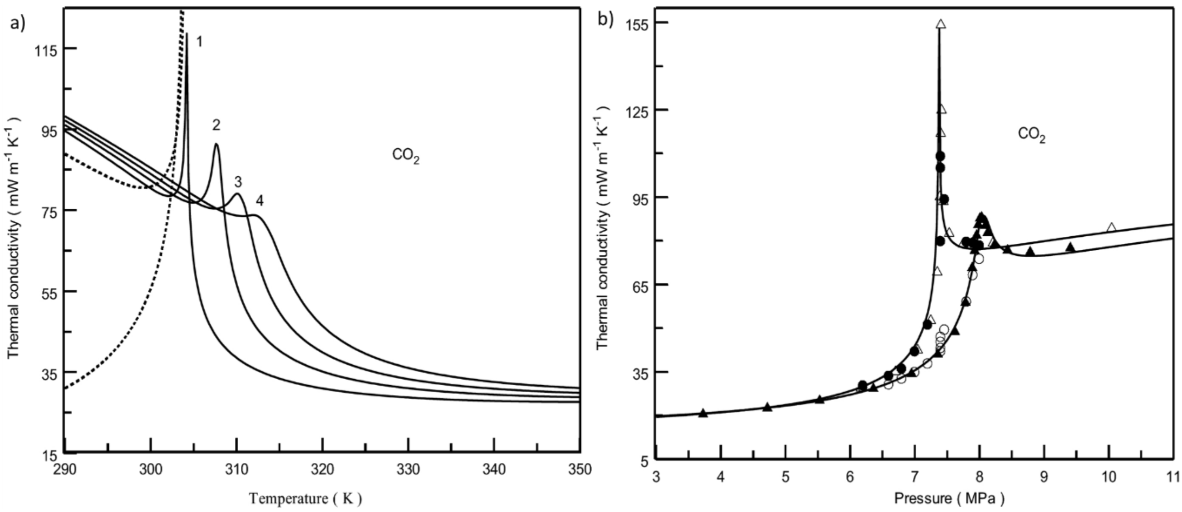

Figure 1 Gradient of thermal conductivity of CO_2 around the critical region. with respect to a) temperature, b) pressure [42].

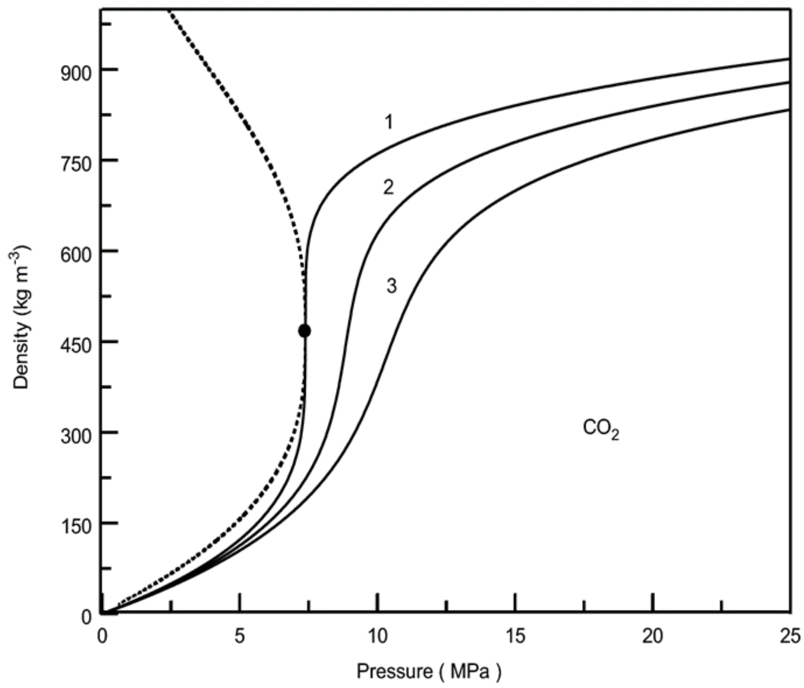

Figure 2 Sudden change of density of CO_2 near the critical region [42].

In supercritical phase the clear boundary that typically separates liquids and gases is not distinguishable. This means that small changes in temperature or pressure can lead to significant changes in density, which in turn affects the thermal conductivity. This can be shown in Figure 3 [42].

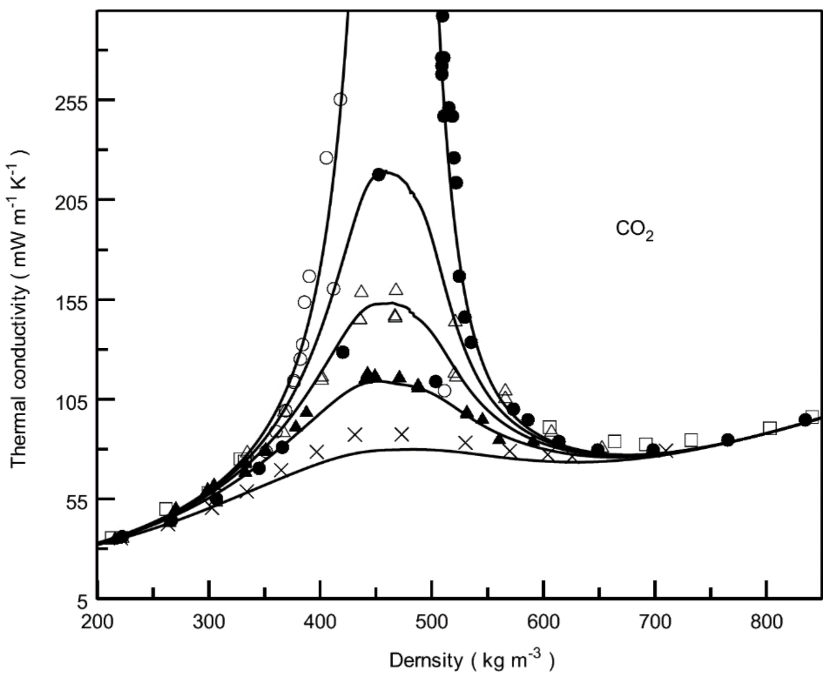

Figure 3 Nonlinear thermal conductivity characteristic of CO2 in relation with density [42].

Crucially, high design pressures are necessary for transcritical operation. CO_2 has a high vapor density and a correspondingly high volumetric heating capacity. This allows a smaller volume of CO2 to be cycled to meet the same heating demand, resulting in smaller components and a more compact system [41]. However, the design and manufacturing complexities of such operating condition previously contributed to CO_2's market decline circa 1940. Today's advanced manufacturing technologies and rich knowledge base have broadened the landscape of optimization of CO_2's attributes in compression cycles [2, 13].

Transcritical CO_2 heat pump systems

Traditional heat pumps operate entirely beneath the critical point of the chosen refrigerant, where the heat is absorbed as the refrigerant evaporates under low pressure, and released when the high-pressure refrigerant condenses. In contrast, transcritical heat pumps diverge in the heat rejection process. Instead of leveraging condensation, the refrigerant pressure exceeds the supercritical threshold, leading to a heat ejection through sensible cooling of CO2 gas [41]. This distinction is visualized in pressure vs enthalpy diagrams in Figure 4. In the transcritical cycle, the conventional condenser is replaced with a gas cooler for heat rejection.

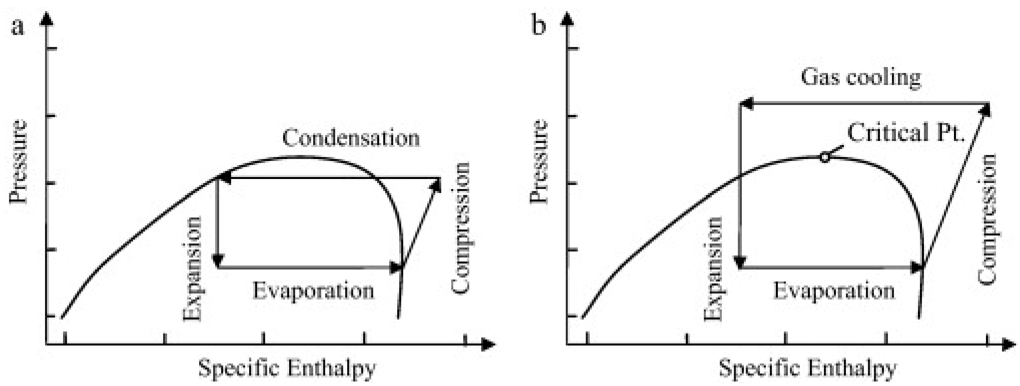

Figure 4 Pressure vs enthalpy diagram of CO2 compression cycle in a) subcritical mode, b) transcritical mode. [41].

In a subcritical heat pump cycle, the low critical temperature restricts the operating temperature range. Heat cannot be delivered at temperatures exceeding the critical temperature. Moreover, at temperatures slightly below, the enthalpy of vaporization decreases, leading to a reduction in heating capacity and system performance. At more elevated heat sink temperatures, transcritical operation becomes requisite. A representative CO_2 process is depicted in Figure 5, illustrating the transcritical CO2 cycle. The heat rejection under supercritical pressure is associated with a sliding temperature instead of a stable condensation temperature [41]. The management of this process necessitates controlling the high-side pressure to achieve peak efficiency.

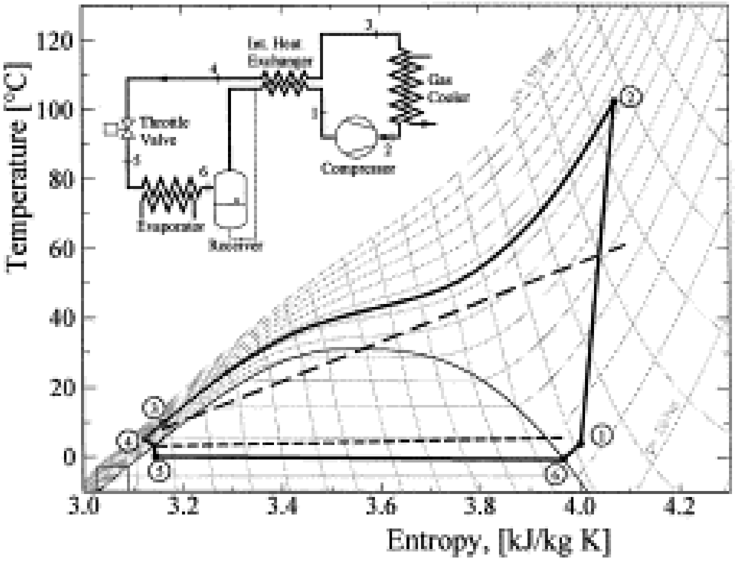

Figure 5 Temperature vs entropy diagram of transcritical heat pump cycle, featuring a sharp temperature glide [43].

The coefficient of performance (COP), for a heat pump is defined as the ratio of its heat rejection capacity and compressor mechanical work input . Figure 6 provides an overview of how heating capacity, COP, and compressor shaft power fluctuate relative to the compressor discharge pressure in supercritical region [41] [43].

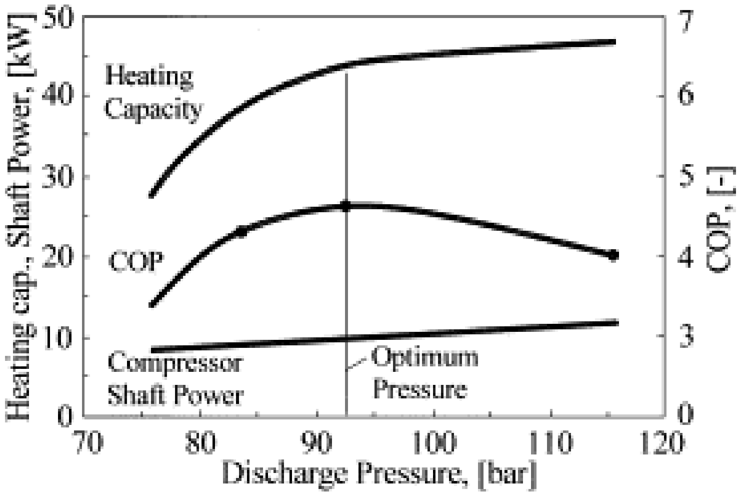

Figure 6 Heat pump performance indicators as a function of discharge pressure [43].

A sharp initial rise in heating capacity can be observed, which subsequently stabilizes at higher discharge pressures. Furthermore, compressor shaft power exhibits a near-linear escalation with discharge pressure. A efficiency peak can be seen at a specific optimum discharge pressure. This variance COP around this optimal region depends on factors such as boundary conditions, the compressor's isentropic efficiency curve, and the configuration of the heat pump system. A comprehensive elucidation is available [43].

In subcritical operation, the efficiency (COP) is primarily confined by the apex of the heat sink temperature. However, in transcritical scenarios, the limiting factor for COP shifts to the minimal refrigerant temperature attainable post heat rejection. In essence, the lowest heat sink temperature sets the boundary. Hence, a heat distribution system with an elevated temperature glide seems favorable for CO2 heat pumps [31]. A common oversight in comparing the energy efficiency of CO2 to other fluids is assuming the same temperature patterns at the cooler's end for both systems. This often disadvantages CO2. A fairer comparison would be to equate the average temperature differences in heat exchangers, ensuring consistent standards for temperature trends [8, 31, 41]. The heat distribution system's design must acknowledge this distinction.

The effective utilization of the transcritical cycle is requires addressing the significant pressure difference and the specific nature of the gas cooling process. Optimization of this cycle requires an understanding of its distinct components and operating parameters. For heating applications that need a considerable temperature increase, the transcritical cycle's proved advantageous compared to the condensation process [41]. In a transcritical CO2 system, the pressure difference between heat rejection and heat absorption is more pronounced than in a typical subcritical system. Additionally, the pressure ratio in transcritical systems is often lower. This lower pressure ratio enhances the efficiency of the transcritical system's compressor [44].

A unique aspect of the supercritical region is the independence of temperature and pressure values. This means that the CO2 temperature post the gas cooler isn't tied to its internal pressure. This temperature is pivotal as it dictates the heat pump's efficiency by determining the heat release amount [8, 41]. Efforts in optimization primarily focus on pinpointing the ideal gas cooler outlet temperature that aligns with the peak operating pressure. Existing correlations that link the heat transfer coefficient and pressure drop in various scenarios are not precise for CO2. For reliable numerical modeling of transcritical heat pump systems that use CO2, accurate correlations to forecast the heat transfer coefficient and pressure drop during supercritical gas cooling, as well as single-phase heating and cooling are needed [45].

Multiple simulations have shown that there's an ideal gas cooler pressure for a specific gas cooler outlet temperature [41].

There are recognized challenges in the CO2 system, including suboptimal heat exchanger design, water temperature complications, and variable system pressures. Despite these challenges, there's potential for refining the CO2 system's performance [46]. It's evident that further advancements in this domain are on the horizon. Recent research underscores the adaptability of trans-critical CO2 cycles, especially for water and air heating applications.

Heat pumps in building heating systems

Refrigeration cycles in buildings are generally used for heating and cooling of either air or water, mainly for the purpose of space heating, and domestic hot water. These two heat rejection mediums present varying heat transfer behaviour in the gas cooler. The same point is valid for evaporator. The heat source of a heat pumps in buildings are commonly air, water, or ground. The operating condition of the heat pump is therefore highly dependent on the characteristics of its source and sink. Heat rejection in supercritical region, as discussed earlier is characterized by a wide temperature glide, making this type of process suitable for high temperature applications. Water heating by traditional heat pumps are restricted to their evaporation temperature, thus could not exceed 55 °C. On the contrary, CO_2 heat pumps are able to deliver up to 90°C water with minor performance degradation. studies on residential transcritical heat pumps suggested promising outcomes [8, 47, 48].

A notable expansion in the market potential for CO2 heat pumps can be envisioned if they can efficiently cater to space heating needs, alongside the already established benefits for water heating. The best performance can only be achieved when the gas cooler outlet is low enough. In building DHW and space heating demands are typically required at temperature different temperature levels. This provides an excellent opportunity to exploit the supercritical CO_2 gas cooling. A system layout for a space and water heating was proposed by [49] as depicted in Fig. 5.

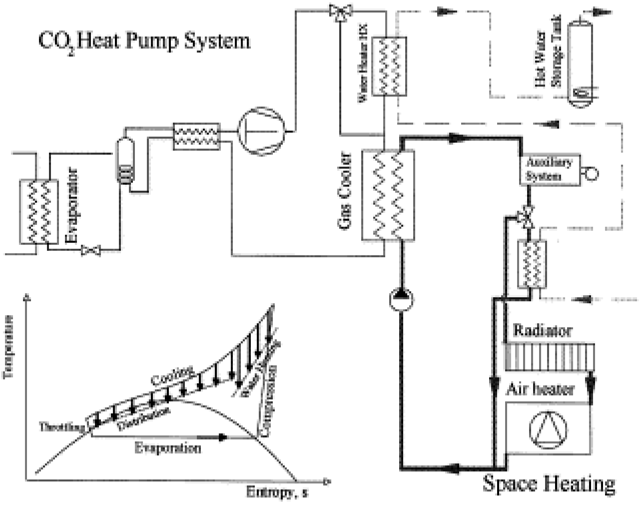

Figure 7 Schematic of a proposed CO_2 heat pump for space heating and hot water [49].

To optimize system efficiency, the design incorporates a series-connected radiator and air heating system. This arrangement aids in ensuring the lowest feasible return temperature. The design also implies a preliminary heating approach for tap water, functioning in parallel with space heating. Tapping into the hot discharge gas facilitates reaching the desired hot water temperature.

Choice of the heat source for the heat pump is a critical design factor, as it determines the heating capacity of heat pump . Besides the resource availability and economic justifications, the desired thermal performance can only be expected when the heat absorption from surrounding is sufficient and reliable for a given operation mode. In general, higher evaporation temperature leads to higher heating capacity. On the other hand, the evaporation temperature is limited by the source. The operation range of CO2 allows for exploiting heat from surrounding as cold as -20°C. Hence, previous studies on transcritical application in buildings mostly investigated the air-sourced heat pump and refrigeration systems. Ground thermal energy has attracted attention during the past decade in all sectors. Ground source heat pumps have been subject of research by many authors, indicating the performance improvements achieved from a more stable and higher temperature source [30, 31, 50, 51].

Ground source heat pumps (GSHPs) exhibited superior performance over traditional air-source HPs, primarily due to the ground's stable temperatures. Heat is drawn from the earths thermal energy capacity in GSHP systems using a ground heat exchanger (GHE) filled with a carrier fluid. Despite considerable research on conventional GSHP systems, their market adoption remained limited due to their initial costs and extended return on investment periods. In more recent times, direct-expansion ground source heat pumps (DX-GSHPs) have seen increased focus. In these setups, refrigerants within the GHE undergo evaporation, directly extracting heat from the soil [30]. A transcritical DX-CO2 GSHP was constructed, and its performance was assessed across three building heating applications, spanning low to high water temperature demands. The findings revealed superior efficiency and capacity in lower temperature demands, with the system's peak COP reached approximately up to 4 during radiant floor heating operation [30].

An experimental study was conducted on a transcritical CO2 air source heat pump (ASHP) paired with thermal energy storage (TES) for residential heating applications. This setup yielded a COP near 20% higher than a standalone air source heat pump. Meanwhile, an equivalent amount of COP reduction was observed when the inlet water temperature at the gas cooler rose. In addition, utilizing a TES, the expansion valve adjustments of heat pump was more efficient, leading to lower expansion losses. An extensive investigation of air heating systems with CO_2 heat pump was performed in [52, 53]. Authors utilized a ground-to-air heat exchange mechanism to preheat the air. This solution yielded a warmer air source for evaporator even in the coldest weather conditions.

In a combined heat pump water heater and space heating application, the gas cooler's partitioning can optimize the temperature profile to closely match that of CO_2, thereby beneficially utilizing the temperature glide. this concept was explored by [54] both experimentally and theoretically. The study found that the COP was highest during combined mode operation, while slightly decreased in only water heating. During the space heating alone the COP was at the lowest. This observation was in contrast with heat pumps using conventional refrigerants, where space heating alone typically achieves the best COP [54].

Previous studies have shown the superior performance of $TCCO_2HP$ water heaters compared to traditional systems. The magnitude of CO_2 charge and expansion valve opening degree were found able to significantly change COP by imposing varying optimal sizing criteria for components of the heat pump, including heat exchange areas [25]. Experimental analyses and simulations of $TCCO_2HPs$ for residential space heating showed that high water temperature entering the gas cooler decreases the COP by increasing the compressor's optimal discharge pressure and the expansion valve losses while utilizing latent thermal storage acting as a sub-cooling device connected to the heating system was found beneficial in terms of overall system COP [55, 56]. Subcooling mechanisms for the gas cooler outlet CO_2 by employing dedicated mechanical subcooling have been proposed in recent research as a potential solution for preventing COP degradation when the return water temperature from the heating system is high [24, 26]. The optimal design of components for a water-sourced $TCCO_2HP$ utilized for domestic hot water generation was investigated through experimental and numerical analysis. It was concluded that for the delivered water temperatures between 35°C to 45°C the optimal discharge pressure was independent of the water temperature at the evaporation inlet. On the contrary, for high-temperature water supply at the gas cooler, the optimal discharge pressure highly varies with the evaporator water inlet [47]. Experimental performance analysis of $TCCO_2HP$ showed the mass flow rate of the hot water at the inlet of the gas cooler affects the optimal discharge pressure, COP, and refrigerant temperature exiting the gas cooler [23, 48]. Controlling the mass flow rate could be an effective method to obtain higher temperatures with a minimal penalty on COP [23]. Moreover, a higher water source temperature could yield significantly higher heating capacity, while increasing COP and the optimal discharge pressure [48].

Given the multivariate performance characteristic of the $TCCO_2HPs$ and the high dependency of the optimal operation on system components, design layout, and real-time operating conditions, conventional control and design optimization methods may not be able to sufficiently adapt to system dynamics when working in the trans-critical region. Hence, the development of optimal control strategies for complex energy systems has become today's research hotspots in this regard [21, 29, 57, 58].

Model predictive control

In essence, the goal of an optimal control problem is to determine a suitable time-dependent input for a dynamic system. This ensures that the system's internal variables trace an acceptable path, all while minimizing a specific performance measure. When solved, these control problems repeatedly in real-time, lay the foundation for control methods grounded in optimization, like MPC [59]. The basic concept of MPC is to use a dynamic model to forecast system behaviour, and to optimize the actuations to operate under the best sequence of decisions (the control move at the current time).

In the context of building energy control and management, MPC plays a pivotal role in ensuring energy efficiency, comfort, and sustainability. Buildings are significant consumers of energy, and their consumption patterns can be highly variable. MPC, with its predictive capabilities, can anticipate energy needs based on occupancy, weather forecasts, and other relevant factors. Thus, it ensures that energy is used optimally, reducing wastage and costs [32, 36, 60-62].

One of the primary objectives in building management is to ensure the comfort of its occupants. MPC can balance energy-saving goals with comfort requirements, such as maintaining optimal temperature and humidity levels. By predicting the thermal behavior of a building, MPC can make proactive adjustments to HVAC systems, ensuring a comfortable environment [32]. As buildings increasingly integrate renewable energy sources like solar panels, there's a need for sophisticated control strategies. MPC can optimize the use of renewables by predicting their output (e.g., solar energy generation based on weather forecasts) and adjusting building operations accordingly [34, 63, 64]. In times of peak energy demand on the grid, buildings can be significant contributors. MPC can participate in demand response programs, where it adjusts building energy consumption in real-time to alleviate grid stress, all while ensuring that comfort and operational needs are met [62, 65, 66]. By optimizing energy consumption patterns, integrating renewables effectively, and participating in demand response programs, MPC can lead to significant cost savings for building operators and owners [67]. To successfully implement MPC for buildings, it is essential to have a dynamic building model that balances accuracy with simplicity. For example, the resistance–capacitance model has been used vastly for its effectiveness in forecasting building thermal dynamics, while remarkably reducing the modelling costs [39].

The operation of heat pumps is strongly dependent on both the outside temperature and on the load. In order to correctly evaluate the performance, the specific applications of the unit need to be properly taken into account. The actual seasonal coefficient of performance (SCOP) is usually different from the one declared in the manufacturer’s data sheets, and other estimations. Moreover, the HP performance is affected by defrosting cycles losses, losses due to the transient after the switch on, and in variable speed units, the COP variation at part load conditions. Neglecting the COP variation at part load operation of variable speed units leads to underrate the performance. However, the information on how the COP varies is rarely declared by the manufacturers and it is thus difficult to correctly simulate a specific market product. Researchers have widely studied the best discharge pressure in transcritical systems. These efforts were dedicated to various operational situations and uses. commonly, researchers tried to determine the precise optimal discharge pressures under different conditions using detailed simulations or tests. This method produced formulas that show the relationship between optimal discharge pressure and operational factors based on repeated trials.

Over the last decade, along with the rise in the market share of CO2 refrigeration cycles, a comprehensive amount of research and development on design and optimal configuration of TCCO2HP. Meanwhile, the pressing need for sustainable building energy system has placed heat pump technologies at the center of most energy conversion system designs for houses. Moreover, the advancement of data processing and numerical analysis techniques during the recent years, numerous advanced control methods including MPC have been proposed to treat the complex energy performance of the buildings [59, 68, 69] . However, only few research was found that addressed the optimization potentials of TCCO2HP performance in the context of building energy systems using MPC techniques [14].

Zhang et al. introduced a predictive control method for CO2 air conditioning in trains, targeting both passenger comfort and energy efficiency. This control adjusted key parameters like discharge pressure and evaporator airflow. The model combined data-driven with physical principles and used a neural network based on detailed operational data. The approach improved energy efficiency in real-time while maintaining comfort. The predictive method was shown to be able to outperform traditional PID control [70].

An ASHP water heater was enhanced using the MPC strategy [57]. Instead of focusing on optimal heat rejection pressure, this strategy used the MPC to predict operational conditions and select the best inputs using a control model. This knowledge came from a detailed model in Dymola. From this, a model suited for MPC was developed. The MPC aimed to improve the water heater's performance coefficient, considering specific formulas and limits. Its effectiveness was tested under various conditions, proving its improved control [57].

3. Methods

1. Theoretical framework

This chapter presents the methods used to establish models for $TCCO_2HP$, building energy dynamics, as well as ground coupled heat exchangers. Further, a MPC controller was designed for the proposed system. The main objective of this research was to explore the extent in which MPC approach could mitigate the operational challenges with TCCO2HP i.e., the loss of heat transfer capacity at off-design conditions which can lead to low COP and poor thermal comfort. The concept of MPC is inherently based on a mathematical model of the process. Previous studies have extensively discussed the effect of model generation method and its complexity on the performance of MPC. Meanwhile, the literature is mostly focused on air sourced TCCO2 system, resulting in well-describing correlations for sizing and performance characteristics. In addition, most studies were performed on the cases with single end-use in a household, either hot water production or space heating. Moreover, while several studies have shown the numerical advantages of black box modelling in facile implementation of MPC in building energy systems, few studies harnessed this approach for the system proposed in this study. For these reasons and due to the lack of adequate data to represent the performance of ground sourced TCCO2HP, especially in the context of residential sector, a white box modelling approach was adopted. MathWorks R2023a software was used to design the proposed system [71]. Simscape was used to construct the time-domain dynamic system model of components. Further Simulink and MATLAB was used to develop control-oriented models and design MPC frameworks. Simscape provides block libraries for simulating physical systems using the acausal physical network approach. Unlike standard Simulink where blocks depict mathematical operations, Simscape allows for the emulation of real-world components. The physical network solver represents systems as functional elements, interacting by exchanging energy through bi ports. This simplifies the modelling process for complex systems. Energy flows are defined by “Through” and “Across” variables with relations defined by physical laws . The methods presented here in this chapter are based on the fundamental conservation equations, namely the conservation equations for mass, momentum, and energy as stated om Equation 3-1 to 3-3, respectively:

$$\frac{\partial \rho}{\partial t} + \nabla \cdot \rho \mathbf{v} = 0 \qquad \text{3-1}$$

$$\frac{\partial \rho \mathbf{v}}{\partial t} + \nabla \cdot \rho \mathbf{v}\mathbf{v} + \nabla \mathrm{p} = 0 \tag{3-2}$$

$$\frac{\partial \rho e}{\partial t} + \nabla \cdot (\rho e \mathbf{v}) = -\nabla \cdot \boldsymbol{q} + F \cdot \mathbf{v} \tag{3-3}$$

Where ρ is density, $\mathbf{v}$ velocity vector, e specific internal energy, $\mathbf{q}$ heat flux vector, F body force vector. Energy conservation can be written in many forms. Often for the fluids in single phase at constant pressure Equation 3 can be written as:

$$\rho c_p(\frac{\partial T}{\partial t} + \mathbf{v} \cdot \nabla \mathrm{T}) = \nabla \cdot (k\nabla T) + \varphi_s \tag{3-4}$$

Where T is temperature, k is thermal conductivity, φ_s energy generation and/or dissipation, c_p Specific heat at constant pressure. For some flows, especially incompressible substances, it might be more convenient to express the energy equation in terms of enthalpy h:

$$\frac{\partial \rho h}{\partial t} + \nabla \cdot (\rho h \mathbf{v}) = -\nabla \cdot \mathbf{q} + F.\mathbf{v} + \varphi_s \tag{3-5}$$

where $h = e + pv$, and v is specific volume. In the process of deriving the Equations 3-1 to Equation 3-5 assumptions are often made to reduce the complexity of the models while maintaining an adequate level of accuracy.

System Description

The proposed residential heating system as shown in Figure 8, consisted of several modern energy equipment. A shallow ground coupled heat exchanger (SGCHEX) was considered as heat absorption mechanism. A TCCO_2HP extracts heat from the ground and delivers to the building for distribution. The user side can be decomposed into units of thermal energy storage, DHW tank, and space heating subsystem. The TCCO_2HP was comprised of 4 primary components of evaporator, compressor, gas cooler, and expansion valve.

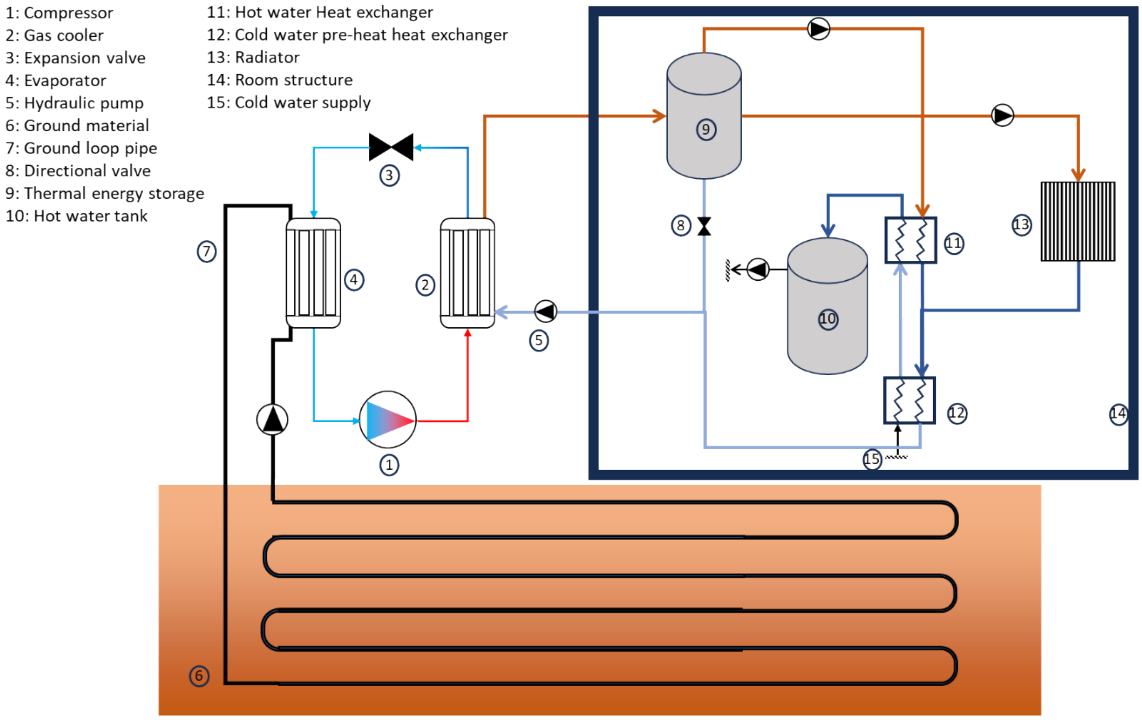

Figure 8 Layout of the proposed $TCCO_2HP$ residential heating system.

Thermal energy storage (TES) (9) was responsible for delivering the heat to hot water tank (HWT) (10) and space heating units (13). In addition, TES was used to act as a buffer, reducing the temperature fluctuations. The heat supply network was in parallel. This was due to generally high supply temperature from the heat pump which was not suitable for direct space heating using a single gas cooler. In the DHW supply path, the hot water was directed into HWT where indirectly rejects heat into the tank volume (11). The return water flows from the space heating joins the return from DHW before returning a pre-heating heat exchanger (12), where the cold water refilling the HWT can cool down the return flow before gas cooler. This configuration was inspired by the system proposed by [49]. This way the return flow to the gas cooler could be cooled down, making the heat transfer in gas cooler more efficient. In addition, this could reduce the temperature variations due to charge/discharge, while maintaining a higher average state of charge in HWT. The flow rate into the gas cooler could be adjusted through a directional valve from TES in the return line (8). Finally, when TES is charged and supply from gas cooler is not needed, the gas cooler flow is blocked and the water loop is between TES and DHW, and SH unit.

2. Thermal model of the building

Modelling the energy dynamics and heat load patterns in buildings can be complex. Nevertheless, there are proven approaches to simplify these interactions by ignoring or aggregating certain thermal effects. The dynamic thermal model of the building was created by considering the conductive and convective heat transfers through the elements of the building, and as a result of their interaction with boundary conditions. A thermal network that encapsulates the dynamic evolution of the average indoor air temperature and mass of the building as a result of exposure to outdoor temperature, heat transfer through the building envelope, infiltration losses and thermal gains due to occupant presence, lightings and equipment can be written as [33, 39]:

$$C_a \frac{dT_a}{dt} = \frac{(T_e - T_a)}{R_{ei}} + \frac{(T_o - T_a)}{R_l} + Q_g + Q_{sh} \quad (3\text{-}6)$$

$$C_e \frac{dT_e}{dt} = \frac{(T_a - T_e)}{R_{ei}} + \frac{(T_o - T_e)}{R_{eo}} \quad (3\text{-}7)$$

Where C_a and $C_e$represent the lumped thermal capacity of indoor air and building envelope. The thermal mass of the windows was ignored due to its negligible contribution to overall capacitance of the envelope. T represents temperatures, R is thermal resistance, Q_{sh} is the space heating added via a radiator. The aggregated gains due to occupancy, equipment, lights and solar radiation gains are included in Q_g. Indices e , a , i , o refer to the envelope measured at midpoint of the element, indoor air measured as average, internal side, and outdoor, respectively. R_l accounts for losses through the window and infiltration. Thermal resistances could be obtained as

$$R = \frac{1}{UA} \quad (3\text{-}8)$$

Here, A is the heat transfer area. The overall heat transfer coefficient U carries the equivalent contribution of conductive and convective heat transfers coefficient as:

$$U = \frac{1}{\frac{1}{h_i} + \frac{\Delta x}{k} + \frac{1}{h_o}} \quad (3\text{-}9)$$

Where h, k, and Δx are the convective and conductive heat transfer coefficients the half of the thickness of the envelope section.

This representation was implemented in Simscape as shown in Figure 9.

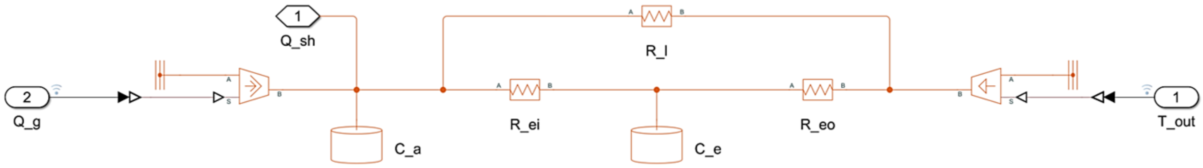

Figure 9 Schematic of Simscape building model.

The space heating radiator unit was modelled as a typical radiator considering the heat transfer between the water flowing in the radiator and indoor temperature. The energy conservation in the radiator can be formulate as:

$$mC_p\frac{dT_{sh}}{dt} = \dot{m}_{sh}C_p(T_{tes} - T_{sh}) + \frac{(T_{sh} - T_r)}{R_{rw}} \quad \text{3-10}$$

$$C_{p_r}\frac{dT_r}{dt} = \frac{(T_{sh} - T_r)}{R_{rw}} + \frac{(T_a - T_r)}{R_{ra}} \quad \text{3-11}$$

Where m is the mass of the water inside the component. C_p is specific heat capacity of water and $C_{p_r}$is capacitance of radiator mass. R_{rw} and R_{ra} are the overall heat transfer coefficient between the radiator and water inside the pipe, and indoor air, respectively. In Equation 3-10, T_{tes} is the temperature of the water from hot water tank. The radiator model in Simscape using pipe and thermal mass blocks is shown in Figure 10.

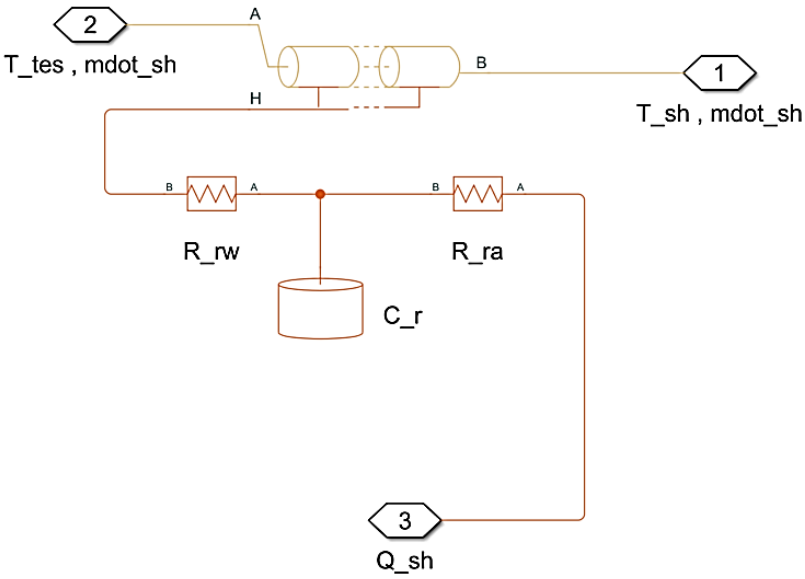

Figure 10 Radiator sub-model in Simscape.

Similarly, the PH-HEX1 and PH-HEX2 ((12) and (13) in Figure 8) were modelled using the same pipe and resistance blocks. Figure 11 shows the arrangement of the two heat exchangers, neglecting the thermal mass of the pipe walls. Cold water with temperature T_0 passes adjacent to the confluence stream from radiator and HWT in PH-HEX1. This would heat the water up to T_{ph}. Then the flow passes through PH-HEX2 which is in contact with return flow from HWT only, this may heat up the supplied hot water even more to $T_{0,feed}$, the temperature at which the tank is filled again.

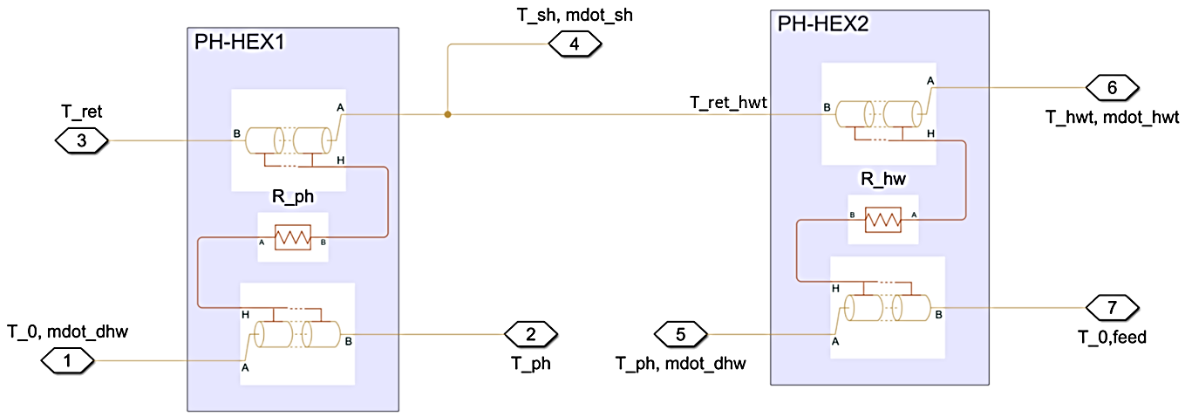

Figure 11 Pre-heating sub-models in Simscape.

Considering the temperature of the pipes as state variables, the dynamic energy conservation for the network of PH-HEX1 and PH-HEX2 can be written as:

$$mC_p\frac{dT_{ph}}{dt} = \dot{m}_{dhw}C_p(T_{ph} - T_0) + \frac{(T_{ret} - T_{ph})}{R_{ph}} \quad (3\text{-}12)$$

$$mC_p\frac{dT_{ret}}{dt} = \dot{m}_{sh}C_pT_{sh} + \dot{m}_{hwt}C_pT_{ret,hwt} - (\dot{m}_{sh} + \dot{m}_{hwt})C_pT_{ret} + \frac{(T_{ph} - T_{ret})}{R_{ph}} \quad (3\text{-}13)$$

$$mC_p\frac{dT_{ret,hwt}}{dt} = \dot{m}_{hwt}C_p(T_{ret,hwt} - T_{hwt}) + \frac{(T_{0,feed} - T_{ret,hwt})}{R_{hw}} \quad (3\text{-}14)$$

$$C_p\frac{dT_{0,feed}}{dt} = \dot{m}_{dhw}C_p(T_{0,feed} - T_{ph}) + \frac{(T_{ret,hwt} - T_{0,feed})}{R_{hw}} \quad (3\text{-}15)$$

Where, $R_{hw}$and R_{ph} are thermal resistances between pipes in PH-HEX1 and PH-HEX2 respectively. indices 0, ph, ret, hwt, sh, dhw, $feed$, refer to fresh water, pre-heated (in PH-HEX1), return to gas cooler, hot water tank, space heating, domestic hot water, HWT feed point, respectively.

The TES was considered in this study as a buffer between hot supply temperature from heat pump and store excess heat. In addition, the HWT contains domestic hot water. models of the HWT were developed by considering the energy balance in the tank as a result of heat fluxes in and out of the container. The HWT was heated by an unmixed charge flow rate from TES as shown in Figure 12.

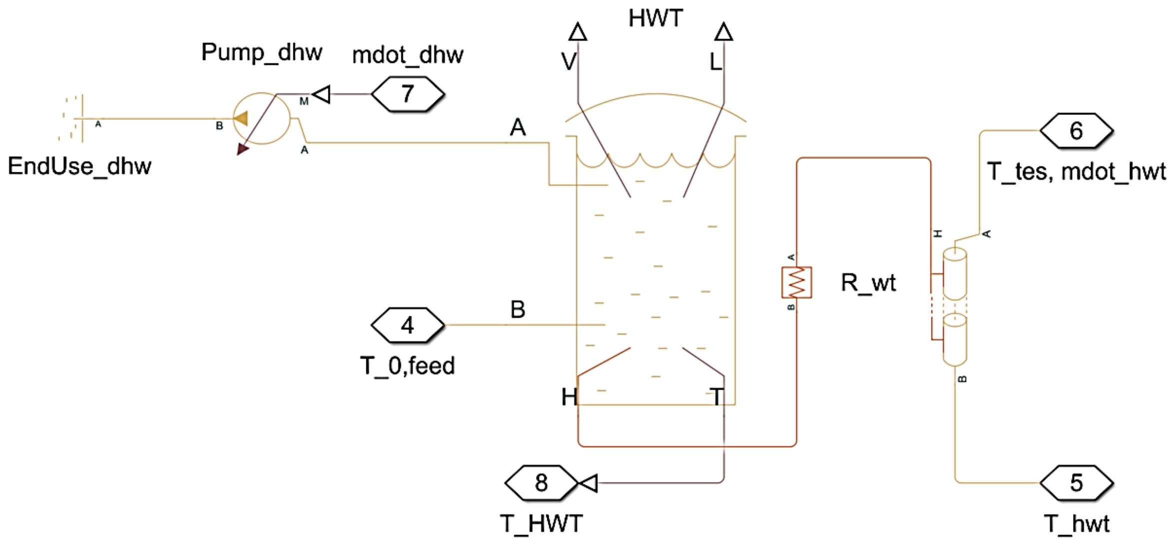

Figure 12 Domestic hot water tank model in Simscape.

This model adopted “Tank (TL)” block from Simscape thermal liquid library. The “Tank (TL)” block assumes a mixed charge/discharge as well as uniform temperature in the tank, neglecting the stratification. Hence, to remedy this limitation the heat added to the HWT was assumed to be in the form of a volumetric heat generation within the tank proportional to the overall heat transfer coefficient and the contact area between the bodies of water in the container and a heat pipe inside the tank. The energy balance for the HWT is established as:

$$m_{HWT}C_p\frac{dT_{HWT}}{dt} = \dot{m}_{dhw}C_p(T_{HWT} - T_{0,feed}) + \frac{(T_{tes} - T_{HWT})}{R_{wt}} \qquad 3\text{-}16$$

where m_{HWT} is the mass of the water in the tank, T_{tes} is the supply temperature from TES, T_{HWT} is the temperature of the tank, R_{wt} is the overall thermal resistance between the pipes passing through the tank and the body of water inside the tank.

for the heat transfer pipe, the energy conservation was written as

$$m_{hwt}C_p\frac{dT_{hwt}}{dt} = \dot{m}_{hwt}C_p(T_{tes} - T_{hwt}) + \frac{(T_{HWT} - T_{tes})}{R_{wt}} \qquad 3\text{-}17$$

Where $m_{hwt}$is the mass of the water in heat pipe. Similarly, TES was designed using the “Tank (TL)” block with governing equation as:

$$m_{tes}C_p\frac{dT_{tes}}{dt} = \dot{m}_{gc}C_p(T_{gc} - T_{tes}) - (\dot{m}_{hwt} + \dot{m}_{sh})C_p(T_{tes} - T_{ret}) - \Delta\dot{m}C_p(T_{tes} \text{ -} \quad \text{3-18}$$

Where T_{gc} and $\dot{m}_{gc}$ is the temperature of the supplied water from gas cooler, respectively. For TES three ports were considered, one that receives the charging heat flow from the gas cooler, one that supplies the heat demand to the end uses, and one connected to the return line to balance the mass flow rates in the tank according to the current demands as:

$$\dot{m}_{gc} + \Delta\dot{m} = \dot{m}_{hwt} + \dot{m}_{sh} \quad \text{3-19}$$

A spool controlled 2-way directional valve was utilized to adjust $\Delta\dot{m}$. The layout of the TES model in Simscape is shown in Figure 13:

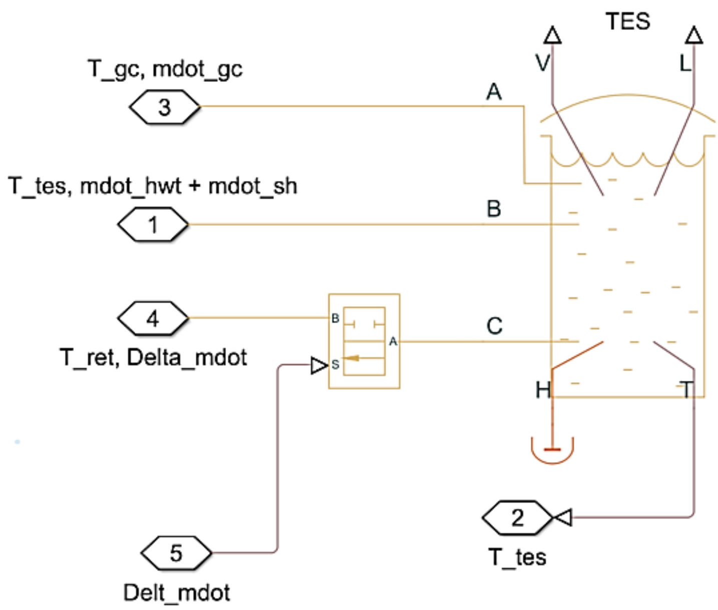

Figure 13 Thermal energy storage tank model in Simscape.

The sub-models of each section were connected to form the whole user side model. The schematic of the building heating substation developed in Simscape is shown in Figure 14. For the distribution of flows 3 circulation pumps were considered. It should be noted that the water was considered incompressible fluid within the working temperature range of this system, hence the momentum balance was simplified by evaluation of hydraulic losses via Darcy-Weisbach relation [72]. It should be noted that both TES and HWT were modelled assuming a constant pressurization in the tank and total dissipation of momentum at the ports. This meant that the pressure levels in the circuit were governed by the tank. This assumption reduced the need for pressure relief valves in the return line, which may not be an accurate representation of the actual system. However, for the purpose of this study, the hydraulic balance was not considered in detail.

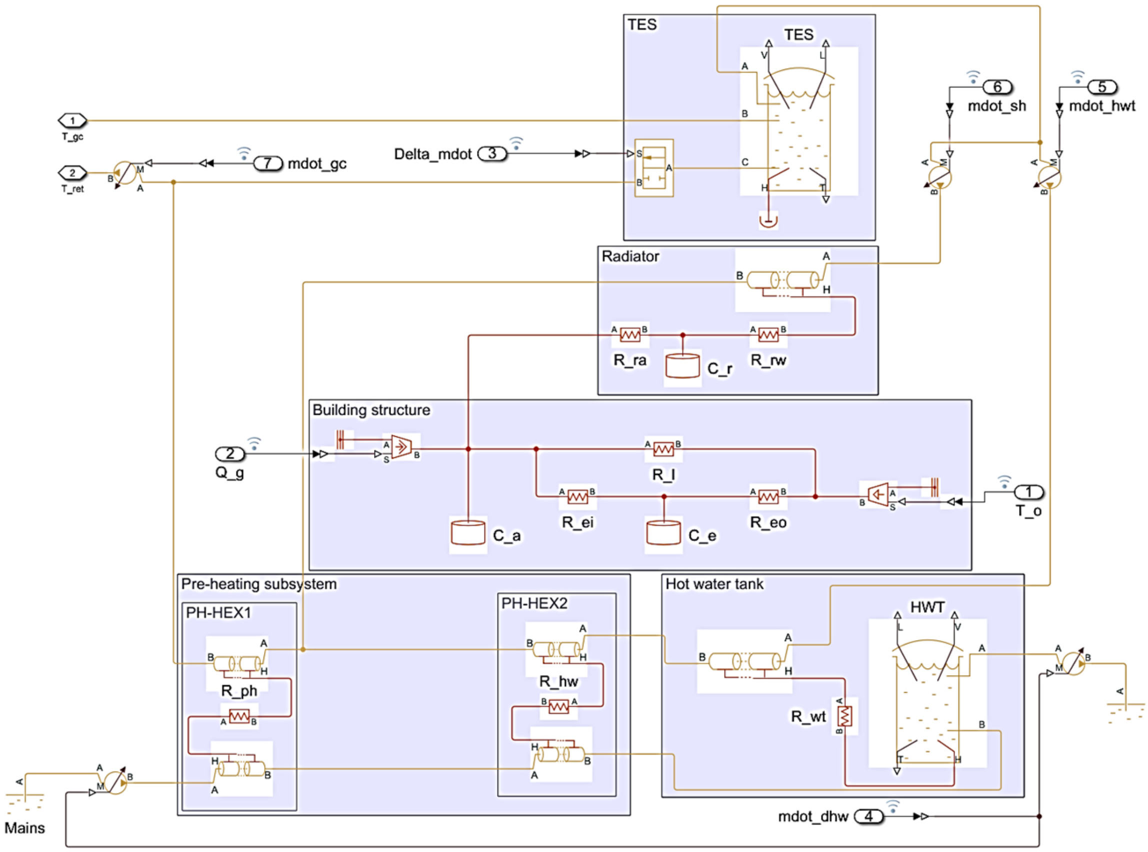

Figure 14 Integrated building dynamic model in Simscape.

3. Trans critical Co2 heat pump

Modelling and analysis of vapour compression cycle could be performed by component-wise thermodynamic analysis of the CO_2 [41, 72]. The TCCO2HP sits at the core of the energy system and its design and operation may have a significant impact on the actual operation of the entire system. Heat pump system for the selected study was a basic design configuration of a vapour compression cycle, though TCCO2HP systems are often equipped with additional components to improve efficiency and robustness, such as internal heat exchanger, vapour injection, multistage compressor. Finding the suitable configuration for TCCO2HP systems, requires a delicate coordinated sizing approach which was beyond the scope of this work. The focus of present study was to model the main 4 components of a generic system that govern the system operation, namely evaporator, compressor, expansion valve, and gas cooler as shown in Figure 15. The reason for this simplification was to investigate they key characteristics of transcritical co2 behaviour, especially the effect of disturbances and MPC on the performance of these components.

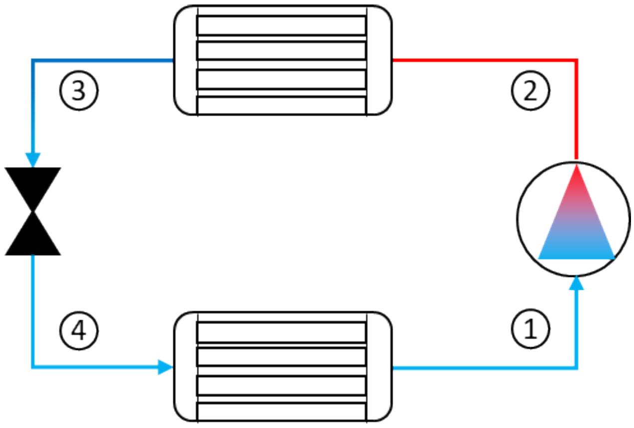

Figure 15 A simple representation of heat pump cycle, pinpointing the process states.

Process dynamics in heat pumps can be very complex and nonlinear. Most of the previous studies considered statistical models based on experimental or nominal operation data provided by manufacturers. Such models are often polynomial representation of heat pump power input, heat rate or COP in terms of cold and hot side temperatures, pressures, or other system variables. these models can significantly reduce the computational burden and has proven reliable near design condition. However, for analysing the dynamic performance of $TCCO_2HP$ achieving an accurate model by these approaches can be challenging.

The physical model of the heat pump system in Simscape was constructed using two "System-Level Condenser Evaporator (2P-TL)" blocks from "Fluids network interfaces" library representing the evaporator and gas cooler, a "Positive-Displacement Compressor (2P)" block, and a custom model of expansion valve. Assumptions included in the heat pump model were 1) adiabatic process in all components, 3) negligible heat and momentum loss between the components, and isenthalpic expansion.

An energy balance equation could characterize every part of the system. The energy balance of a heat pump, assuming isenthalpic expansion and no accumulation of mass in the compressor can be given in Equations 3-20 to Equation 3-24 [73] . Indices refer to Figure 15.

$$\frac{dh_1}{dt} = \dot{m}_{co_2}(h_4 - h_1) + Q_{ev} \qquad 3\text{-}20$$

$$\dot{m}_{co_2}(h_1 - h_2) = W_{comp} \qquad 3\text{-}21$$

$$\frac{dh_3}{dt} = \dot{m}_{co_2}(h_2 - h_3) - Q_{gc} \quad 3\text{-}22$$

$$h_1 = h_4 \quad 3\text{-}23$$

$$Q_{gc} = Q_{ev} + W_{comp} \quad 3\text{-}24$$

where $h = e + \frac{P}{\rho}$ is enthalpy of the fluid, Q_{gc} is the heat rate at the gas cooler, Q_{ev} is the evaporator heat absorption rate from the source, and W_{comp} the compressor power input. Finally, the COP can be defined as:

$$COP = \frac{Q_{gc}}{W_{comp}} \quad 3\text{-}25$$

Heat exchangers

Performance of the gas cooler is highly correlated with the secondary side water temperature levels and flow rates. Given the higher overall heat transfer coefficient of water comparing to CO2, the heat transfer regime in the gas cooler is more sensitive to co2 than water. For example, in a counter flow arrangement reducing the temperature difference between the two fluids at the gas cooler outlet (water inlet, co2 outlet) can reduce the optimum discharge pressure [41].

Design and simulation of TCCO2HP requires an accurate representation of co2 properties in order to capture the dynamic evolution of thermodynamic states in the heat pump cycle. In Simscape two-phase fluid domain, thermodynamic properties can be calculated by means of partial differentiation of equations of states with respect to known state properties. For gas cooler and evaporator, the mass balance contains the derivative of density with respect to time, as well as pressure and internal energy for a discretized control volume along the flow path. Using the chain rule, the mass continuity for the co2 in gas cooler and evaporator is formulated as

$$\frac{\partial \rho}{\partial t} = \left.\frac{\partial \rho}{\partial P}\right|_e \frac{dP}{dt} + \left.\frac{\partial \rho}{\partial e}\right|_P \frac{de}{dt} \quad 3\text{-}26$$

where e is specific internal energy of the fluid, P is the pressure.

Further, the energy conservation for the gas cooler can be written as

$$\frac{dh_3}{dt} = \dot{m}_{co_2}(h_2 - h_3) - Q_{gc} \quad 3\text{-}27$$

Given that the gas cooler unlike condenser operates with a high temperature glide, the actual heat transfer in a heat exchanger can occur along the path as well as in radial direction. However, previous numerical studies showed that the first one is negligible [41]. Hence, the net rate of heat transfer between two fluids in a heat exchanger can be calculated as:

$$Q_{gc} = UA_{gc}\Delta T_{gc} \tag{3-28}$$

Where UA_{gc} is the overall heat transfer conductance of co2, and $\Delta T_{gc}$is the temperature difference between co2 and water in the gas cooler. This term depends on the flow arrangement and the dynamic state of the heat exchanger. For a typical counter flow arrangement ΔT_{gc} is often defined as logarithmic mean temperature difference between the hot and cold side. It should be noted that the Equation is valid in the steady state condition. In general, neglecting the thermal mass of the pipe walls, the energy conservation for the water side of the gas cooler can be derived as:

$$m_{hp}C_p\frac{dT_t}{dt} = \dot{m}_{hp}C_p(T_{tr} - T_t) + Q_{gc} \tag{3-29}$$

Where m_{hp} is the mass of the water in the gas cooler, T_{tr} is the return temperature from the building substation.

The model of evaporator was similar to gas cooler in terms of formulation of mass and energy conservation. Previous research on TCCO2HP have addressed the design considerations for the evaporator in such systems. the heat transfer in the evaporator can be found as

$$Q_{ev} = UA_{ev}\Delta T_{ev} \tag{3-30}$$

In evaporator co2 undergoes phase change at constant temperature. This change in specific volume strongly affects the actual heat absorbed by the fluid. Hence, for the mixed phase region the U value must take into account the effect of latent heat of evaporation. The value of U as given in Equation depends on the number of transfer units (NTU) and flow regime

$$UA_{ev} = Nuk \tag{3-31}$$

Where D_h is the hydraulic diameter of the tube and Nu for a single-phase fluid is a function of Reynolds and Prandtl numbers. When calculating the UA_{ev} in two-phase region, the Cavallini-Zecchin correlation is added that considers the effect of density gradients with respect to saturation density as well. The dynamic energy conservation at the liquid side of evaporator can be written similar to gas cooler as:

$$m_{evap}C_{p,b}\frac{dT_{br}}{dt} = \dot{m}_b C_{p,b}(T_{bs} - T_{br}) - Q_{ev} \quad \text{3-32}$$

where, T_{br} is brine temperature at the outlet of evaporator, $\dot{m}_b$ is the mass flow rate of brine, and T_{bs} is the supply temperature from the ground. Finally the pressure loss in the heat exchangers can be calculated using a simplified Darcy friction equation as

$$\Delta P = f\frac{\dot{m}_{co_2}^2 L}{2\rho D_h {A_s}^2} \quad \text{3-33}$$

Where f is the Darcy-Weisbach friction factor depending on the surface roughness and flow regime, L is the length of the flow path in the component, and A_s is the cross-section area of the pipe.

Compressor

In TCCO2HP reciprocating compressors are commonly used. This is because of their suitability to handle high pressures and have better performance with varying loads [41]. The compressor work can be calculated as

$$W_{comp} = \frac{W_{comp,is}}{\eta_{is}\eta_m\eta_v} = \dot{m}_{co_2}(h_2 - h_1) \quad \text{3-34}$$

Where $W_{comp,is}$ is the isentropic work and η_{is} is isentropic efficiency of the compression process. η_m and η_v are mechanical and volumetric efficiencies. Mechanical efficiency is related to friction losses in the rotary components of the compressor and is often reported between 0.65-0.8. volumetric efficiency is a function of leakages, compressor chamber clearance, and rotation speed, and pressure ratio [73]. The mass flow rate of CO2 is determined as

$$\dot{m}_{co_2} = \eta_v \omega V_d \rho_1 \quad \text{3-35}$$

Where n is the rotation speed, V_d is the displacement volume of the chamber, and ρ_1 is the density at suction port. Both volumetric and isentropic efficiencies depend on the compressor pressure ratio (r). Their calculations stem from the standard operating conditions.

The Positive-Displacement Compressor (2P) block exemplifies a quasi-steady positive-displacement compressor. This means, the accumulation of mass in the chambers was not taken into account. The actual positive displacement compression process is interpreted as polytropic, maintaining the relation of

$$Pv^n = constant \tag{3-36}$$

Where n represents the polytropic exponent. Relying on the polytropic pressure-volume correlation, the block computes the volumetric efficiency using:

$$\eta_v = 1 + \alpha - \alpha(\beta^{\frac{1}{n}}) \tag{3-37}$$

Where the clearance fraction α can be calculated from the compressor design specification as:

$$\alpha = \frac{1 - {\eta_v}^*}{(\beta^*)^{\frac{1}{n}} - 1} \tag{3-38}$$

Where β is the pressure ratio, and asterisk denotes the nominal values. Finally the mechanical energy balance in the compressor is found by equating the mechanical and compression work on the fluid to derive the power input

$$W_{comp} = \frac{1}{\eta_m}\frac{n}{n-1}\eta_v P_1 V_d\left(\beta^{\frac{n-1}{n}} - 1\right)\omega \tag{3-39}$$

Expansion valve

The thermodynamic model of expansion valve was constructed as:

$$h_1 = h_4 \tag{3-40}$$

In order to respect the isenthalpic process assumption at all conditions, a custom component was created in the two phase fluid domain. The block takes the opening ratio AR to calculate the pressure drop across the valve as:

$$\Delta P = AR\frac{\Delta P^*}{\dot{m}^{*}_{C_{02}}{}^{2}}\dot{m}^2_{Co_2} \tag{3-41}$$

Where ΔP is the pressure drop across the valve. Asterix superscript denotes the nominal values at full open position. The layout of the $TCCO_2HP$ in Simscape is shown in Figure 16. It should be noted that the flow arrangement in heat exchangers are defined in block parameter configurations and the connection ports do not represent the actual flow path. As explained in the next section, connection ports T_{br}, and T_{bs} are temperatures associated with the inlet and outlet connections of brine fluid to the ground loop circuit.

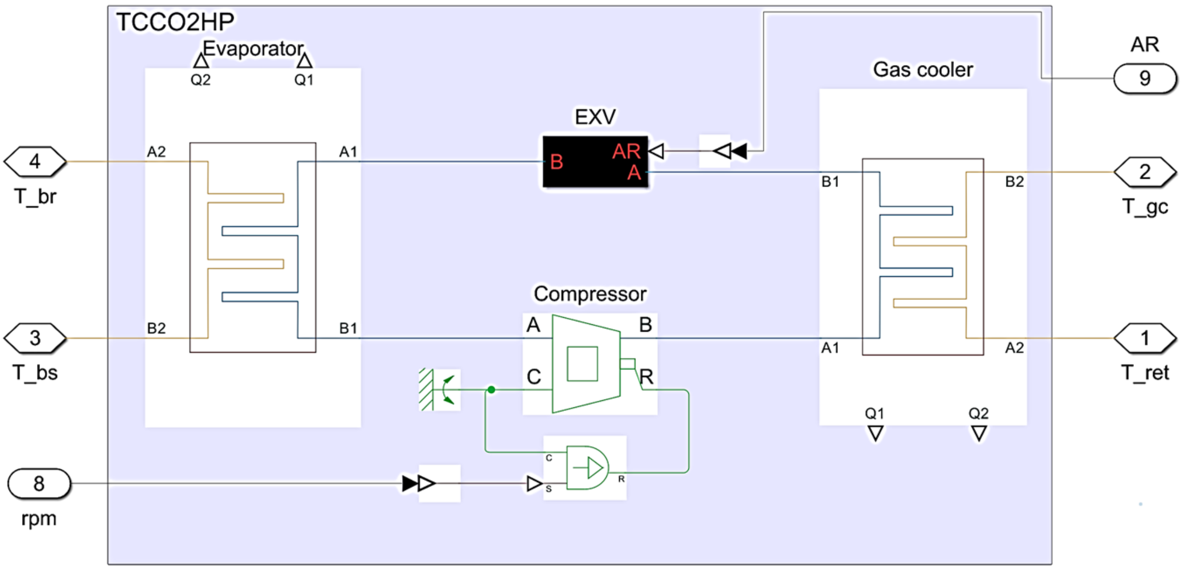

Figure 16 Model of TCCO2HP in Simscape.

4. Ground coupling model

Ground was considered as the heat source for the ground heat exchanger in this study. This configuration has extensively been proposed and applied in many residential heating systems. Ground coupled heat pumps take advantage of more stable ground temperature from at least below 2 meters. Besides, on average ground is cooler and warmer than air during the summer and winter, respectively. This provides a reliable and abundant low grade heat source that can be harnessed by suitable heat pump design.

Design and modelling of ground source heat pumps GSHP requires detailed survey of the site area and ground thermos-physical properties to assess the suitable design and sizing procedure. Depending on the objective and characteristics the energy systems design, ground coupling could be via deep boreholes encompassing fluid channels or shallow piping loops placed horizontally in a trench where the depth of the pipes are no more than few meters below the ground. Shallow GSHP are increasingly considered for residential systems, especially in rural areas where the land is more available. A study tested a U-shaped HDPE pipe, 2.5 m deep and 36 m long, for the HGHE. The TRT recorded a ground thermal conductivity of 0.72W/m·K, aligning with the sandy loam soil at the test site [74].

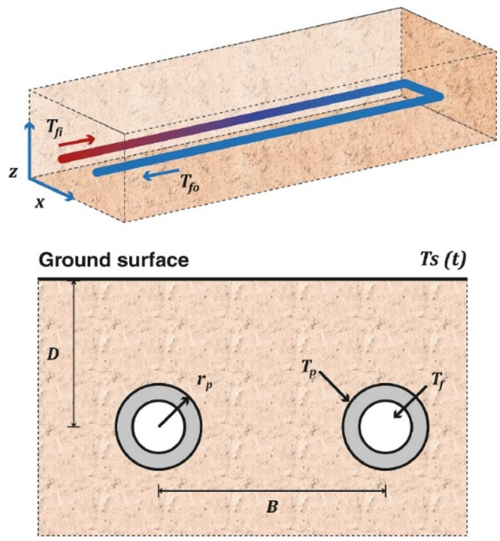

Figure 17 Lyaout of a U shape horizontal ground pipes [74].

A simplified model of a GSHP, suitable for the configuration studied by [74] can be derived from the energy balance between the mass of the soil within the field encompassing the pipes and the brine fluid inside the pipes. The energy conservation for the mass of the ground can be written as

$$m_b C_{p,b} \frac{dT_{bs}}{dt} = \dot{m}_b C_{p,b}(T_{br} - T_{bs}) + 2\pi k_g \frac{L}{\ln\left(\frac{D_o}{D_i}\right)}(T_g - T_{bs}) \quad \text{3-42}$$

$$m_g C_{p,g} \frac{dT_g}{dt} = k_g \frac{A_g}{s}\left(T_g - T_{g,sur}\right) - 2\pi k_g \frac{L}{\ln\left(\frac{D_o}{D_i}\right)}(T_g - T_{bs}) \quad \text{3-43}$$

Where subscripts g and b refer to the ground and brine fluid. D_i is the diameter of the pipes and D_o is the outer diameter of the trench field between the pipe and the surrounding. The models in Equation 3-42 and Equation 3-43 was built in Simscape using “Thermal mass” block to represent the ground material, “conductive heat transfer” blocks for inner and outer portions of the ground material, and “pipe (TL)” block to represent the heat pipes. In addition, a mass flow rate source was used to maintain the circulation. This sub-model can be seen in Figure 18.

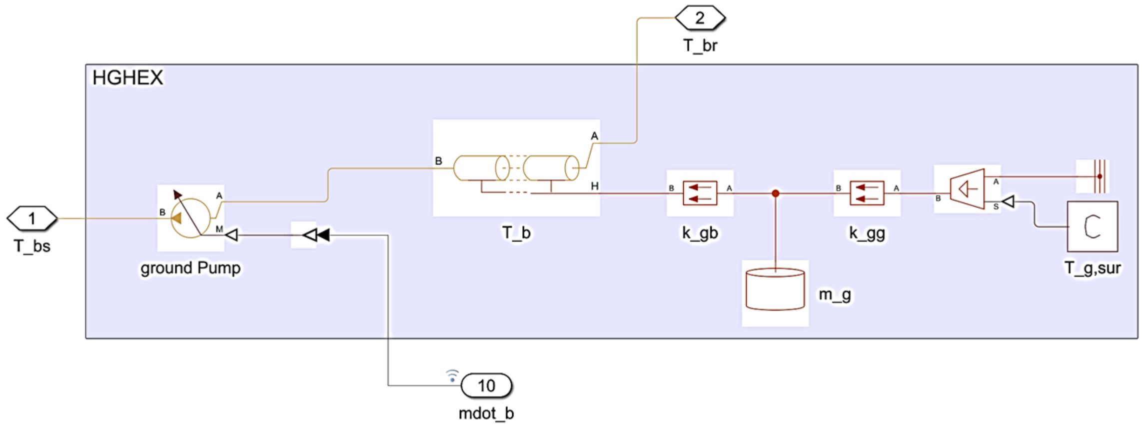

Figure 18 Ground heat exchanger model in Simscape.

The model of all sub-systems presented in previous sections were integrated to establish the full scale physical system model. As shown in Figure .

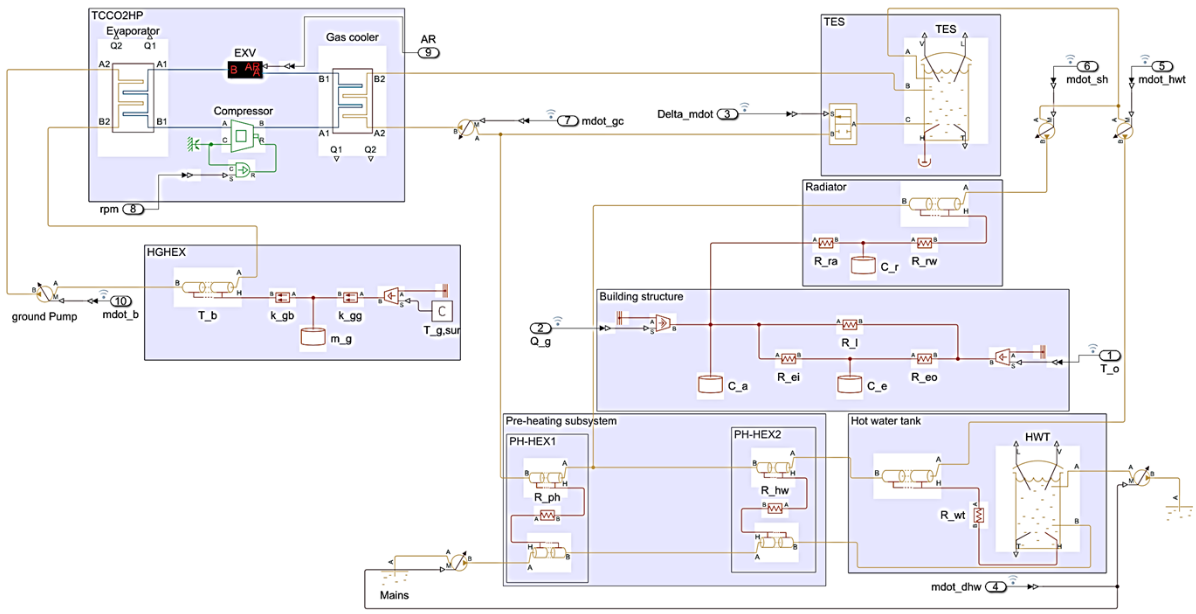

Figure 19 Complete physical model of the TCCO2HP rsidential heating system in Simscape.

The model of the heating system described in previous section was derived in Simscape as a system of ordinary differential equations (ODE) with 18 distrinct state variables that can be described through. Further quasi-static component models such as the entire thermal liquid network of water and ground brine, as well as compressor, expansion valve, pumps, valve, sink and sources were coupled with the system of equations as differential algebraic equation (DAE), enforcing physical relations. Despite its convenience for representing the physical world, systems built in Simscape tend to be nonlinear by nature. These nonlinearities are due to varying actual heat transfer coefficients, gradients of fluid properties and interaction of components in the system. Moreover, some blocks contain additional intermediate states such as temperature states along the length of the heat exchangers and pipes, as well as volume of the tanks. These added up to 65 number of states variables. In general, these equation can be represented by the following state space representation of differential equations:

$$\dot{x}(t) = f(x(t),u(t)) \tag{3-44}$$

$$y(t) = g(x(t),u(t)) \tag{3-45}$$

where $x(t)$ represents the state vector, $u(t)$ denotes the input variables, namely the compressor rotation speed (n) , valve opening degrees (AR and $\Delta\dot{m}$), mass flow rates through the system ($\dot{m}_{gc}$, $\dot{m}_{hwt}$, $\dot{m}_{sh}$). $y(t)$ stands for any measured output represented as a function of states and inputs. To apply MPC to such systems, an understanding and subsequent transformation of these nonlinearities is crucial. Next section presents the intricate process of transforming a nonlinear dynamic physical model, constructed in Simscape, into a simplified, yet representative, linear state space model.

5. Control-oriented system model

Prior to any linearization, it was essential to pinpoint an operating point, which is fundamentally a steady-state condition of the system. Mathematically, this is where $\dot{x}(t)$=0 for a given $u(t)$. From a physical perspective, this operating point implies a scenario wherein the system remains static, not evolving over time, with the effects of disturbances and inputs being in equilibrium. The next phase involves linearization, where the nonlinear system undergoes an approximation using a linear system through the method of Taylor series expansion, limiting the representation to only the first-order terms. This procedure is performed around the desired operating point.

6. Prediction model

As mentioned earlier, the state-space model represents the behavior of the system in terms of a set of state variables and a set of input variables. Based on description of the system in the previous section, the system of linear time invariant (LTI) system of equations was developed.

The model of a residential heating system based on TCCO2HP can be highly nonlinear and complex as it was shown in previous chapter. It was revealed that the heat pump performance can significantly vary by considering different boundary conditions and control decisions. These involved possibility of controlling 1) the distribution pumps in the user substation, 2) heat pump's compressor speed, and 3) controlling the heat pumps expansion valve. The choice of controlled components and its manipulated variable depends on the goal of the control problem.

For example, a necessary practice in heat pumps is controlling the temperature of the refrigerant at the compressor inlet to a slightly superheated temperature. This is to ensure the compressor's mechanical safety by preventing liquid to enter the compressor which can damage the component. Superheating at evaporator outlet is often controlled by adjusting the pressure drop at the expansion valve to match the desired evaporator outlet condition. In this case the valve opening area is a manipulated variable which changes the pressure at the evaporator outlet, leading to a controlled output temperature.

Control methods often use mathematical representation of the studies system by identifying the input signals and measured output relations. For this reason often the control models described as time invariant models in state space form, transfer function, or zero-pole gain formulations.

A linear state space model in its generic form can be written as:

$$\dot{X} = AX + BU \quad \text{3-36}$$

$$Y = CX + DU \quad \text{3-37}$$

Where A, B, C, and D are matrix of constant containing the dynamic behavior of the system via its parameters. Considering a continuous system, Equation 36 and Equation 37 transforms Equation and Equation into:

$$\dot{x}(t) = Ax(t) + Bu(t) \quad \text{3-38}$$

$$y(t) = Cx(t) + Du(t) \quad \text{3-39}$$

Where X are states, U are inputs, and Y are outputs observed in the system. States are variable that define the dynamics of the system, such as temperature, pressure , enthalpy, etc. at different points of the system. Inputs are manipulated and nonmanipulated variables. Manipulated variables are also called control variables include rotation speed and mass flow rates. Outputs must be defined according to the control problem at hand. In this case the general idea is to control the heat pump operation at optimal level while meeting thermal demands. This can be interpreted as controlling COP and costs for heat pump operation, which can be manipulated by changing rotation speed and flow rate of how water in the building to the desired level.

Linearization

The state space model in previous equation describes a linear formulation of an ODE in which the time derivative of states are calculated from current state values and inputs. Further the outputs are defined as linear effect of current states and inputs. However, thermal energy system, especially the model described in previous section is nonlinear, due to dependency of certain input parameters on state variables. For example, assuming mass flow rate as input and temperature as state, the advection heat transfer due to flux of energy in and out of each component could be expressed as:

$$\dot{X} = AX + BUX \tag{3-40}$$

The above equation is nonlinear, because derivative of a state depends on the product of that state to the input. These nonlinearities can be captured by a nonlinear MPC controller, however the computational and structuring the suitable prediction and optimization algorithm can be challenging. Hence, the linearization process can be used as an alternative. The idea of linearization is to locate an operation point and consider the behaviours of the system linear within a finite range. This can yield a relatively accurate approximation of the real system, only in that operating point. On the other hand, handling this linearized model is much easier to handle.

The linearization process can be seen as a special case of Taylor's theorem, which states that any sufficiently smooth function can be approximated by a polynomial of sufficiently high degree. Specifically, the linear approximation obtained through the process of linearization corresponds to the first-order term in the Taylor expansion of the function around the operating point. The Taylor expansion of a function f(x) around a point x0 can be expressed as:

$$f(x) = f(x_0) + (x - x_0)f'(x_0) + (\frac{1}{2!})(x - x_0)^2 f''(x_0) + \dots + \frac{1}{n!}(x - x0)^n f^n(x_0) + \tag{3-41}$$

where $f'(x_0)$, $f''(x_0)$, to $f^n(x_0)$ are first, second to n[th] derivative of $f(x)$ evaluated at x_0, The remainder term $Rn(x)$ represents the error between the true function and its Taylor expansion, and it can be expressed in terms of the higher-order derivatives of f(x). When only the first-order term is considered in the Taylor expansion, a linear approximation can be obtained as:

$$f(x) \approx f(x_0) + (x - x_0)f'(x_0) \tag{3-42}$$

In the case of a multivariate function in the form of $f(x_1,x_2,\ldots x_n)$, as in case of the system in this study, the linearization process involves finding the Jacobian matrix of the function at the operating point. The Jacobian matrix is a matrix of partial derivatives that describes the rate of change of each component of the function with respect to each of the input variables. The linear approximation of the function around the operating point can then be expressed as a matrix multiplication of the Jacobian matrix J_f and the deviation of the input variables from the operating point. This is mathematically structured as:

$$f(x) \approx f(x_0) + J_f(x_0)(x - x_0) \tag{3-43}$$

Where, the Jacobian Matrix is calculated as:

$$J_f(x) = \begin{bmatrix} \frac{\partial f_1}{\partial x_1} & \cdots & \frac{\partial f_1}{\partial x_n} \\ \vdots & \ddots & \vdots \\ \frac{\partial f_n}{\partial x_1} & \cdots & \frac{\partial f_n}{\partial x_n} \end{bmatrix} \tag{3-44}$$

Discretization

Discretization is the process of converting a continuous-time state-space model into a discrete-time state-space model, which can be used for simulation, control, and analysis purposes. The process involves approximating the continuous-time model with a discrete-time model that captures its essential dynamics over a finite time interval. To discretize the described state space model model, a sampling time Ts which represents the time interval between consecutive samples of the system was chosen. Then the continuous-time model and be approximated over this time interval by using a numerical integration method, such as the Euler method or the Runge-Kutta method. The simplest method for discretizing a continuous-time model is the zero-order hold (ZOH) method, which assumes that the input u is held constant over each time interval Ts. In this case, the discrete-time state-space model can be expressed as:

$$x[k+1] = Ad\,x[k] + Bd\,u[k] \quad 3\text{-}45$$

$$y[k] = Cd\,x[k] + Dd\,u[k] \quad 3\text{-}46$$

where Ad, Bd, Cd, and Dd are the discrete-time equivalents of the continuous-time matrices A, B, C, and D, respectively. This process was streamlined from Simscape directly to Simulink Control Design toolbox using "linearizer" function to extract the linearized state space model of the system. Having established a linear representation, the stage is set for the implementation of Model Predictive Control (MPC). To execute this in the context of Simscape, an array of built-in tools, including QP solvers was leveraged, ensuring efficient and optimized control.

7. Model predictive control design

In discrete time, the MPC is formulated as an optimal control problem. The goal of the proposed MPC was to maintain thermal comfort for the user, while optimizing the performance of TCCO2HP. The flow chart in Figure 20 shows the MPC mechanism adopted in this study.

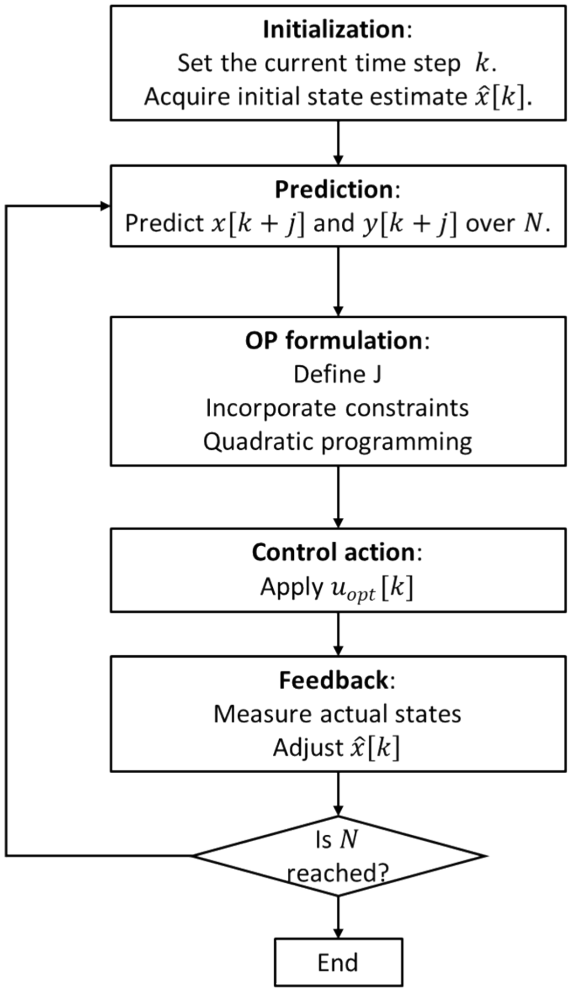

Figure 20 Flow chart of the MPC mechanism.

8. Objective function

The heart of the MPC is its objective function, which quantifies the control goals. For the TCCO2HP system, the objective function $J(u,x)$ was formulated to balance multiple objectives:

$$min\, J(u,x) = \sum_{j=0}^{N} w_1(T_a - T_{a,ref})^2 + w_2(T_t - T_{t,ref})^2 - w_4 COP \tag{3-47}$$

Where w terms are weights that define the relative importance of each objective with respect to others. The first two terms contain the thermal comfort tracking goals set by reference signals $T_{a,ref}$ and $T_{t,ref}$. Typically reference set points could be between 20-22 °C for indoor temperature and 55-70 °C for DHW. The first two terms are standard reference tracking objectives for maintaining the temperature to drive the system outputs towards $T_{a,ref}$ and

$T_{t,ref}$. The last term seeks to maximize COP. The MPC operates within a set of constraints that reflect the physical and operational limits of the TCCO2HP system:

- Operational Limits: Constraints on compressor speed, mass flow rates, and valve positions ensure the system operates within safe and efficient bounds.
- Thermal Comfort: Soft constraints on thermal outputs ensure that the system adheres to established comfort standards.
- Supercritical Operation: A constraint on the compressor's discharge pressure ensures the system operates in a supercritical regime.
- System Dynamics: The state-space representation of the TCCO2HP system imposes inherent constraints on how the system evolves over time.

9. Prediction and optimization

In an MPC, the prediction horizon is used to predict the future values of the state and output variables. These predictions are used to calculate the optimal inputs for the system at each time step. The prediction method involves recursively solving a set of optimization problems over the prediction horizon. The prediction horizon is defined as the length of time over which the MPC predicts the future behavior of the system.

Let k be the current time step. The prediction of future values of the state and output variables over the next N steps constituting the prediction horizon is required. this can be done by recursively solving the following optimization problem:

minimize J

subject to:

$$x[k+j+1] = Ax[k+j] + Bu[k+j], \qquad j = 0,1,\ldots,N-1 \tag{3-48}$$

$$x[k] = \hat{x}[k] \tag{3-49}$$

$$y[k+j] = Cx[k+j] + Du[k+j], \qquad j = 0,1,\ldots,N-1 \tag{3-50}$$

$$x_{min} <= x[k+j] <= x_{max}, \qquad j = 0,1,\ldots,N-1 \tag{3-51}$$

$$u_{min} <= u[k+j] <= u_{max}, \qquad j = 0,1,\ldots,N-1 \tag{3-52}$$

where $\hat{x}[k]$ is the estimated state vector at time k based on the previous measurements, and $x[k+j]$, $u[k+j]$, and $y[k+j]$ are the predicted state, input, and output vectors at time

$k + j$, respectively The constraints are the same as before. The solution of the optimization problem provides the optimal input sequence over the prediction horizon:

$$u_{opt}[k], u_{opt}[k+1], \ldots, u_{opt}[k+N-1] \quad 3\text{-}53$$

The first input in the sequence, $u_{opt}[k]$, is applied to the system, and the optimization problem is solved again at the next time step, $k + 1$. This process is repeated at each time step. The predicted state and output vectors can be calculated using the optimal input sequence and the state-space model as:

$$x[k+j+1] = Ax[k+j] + Bu_{opt}[k+j] \quad 3\text{-}54$$

$$y[k+j] = Cx[k+j] + Du_{opt}[k+j] \quad 3\text{-}55$$

where $Bu_{opt}[k+j]$ and $Du_{opt}[k+j]$ are the portions of the input vector and output vector, respectively, that are determined by the optimal input sequence. The feedback control law is then used to adjust the optimal inputs to account for any discrepancies between the predicted and measured state and output variables:

$$u[k+j] = u_{opt}[k+j] + K_j(x[k+j] - \hat{x}[k+j]) \quad 3\text{-}56$$

where K_j is the feedback gain for time step $k + j$, and $\hat{x}[k+j]$ is the estimated state vector at time $k + j$ based on the previous measurements.

4. Simulation case study

1. Sizing of the components

The models developed in previous chapter were utilized to design and simulate a typical residential heating system using TCCO2HP and MPC. The building model created in this section were based on a typical case of a single-zone heated room. The building was subjected to thermal loads of domestic hot water and space heating in the context of Oslo, Norway. A basic model of the building structure and energy performance was developed in IDA ICE, a software specialized in modelling and simulation of building energy and indoor climate projects. The building structure as shown in Figure 21 and its energy profile were gathered from a standard IDA ICE climate database based on ASHRAE 2003. The construction material and energy standards were chosen, adhering to the Norwegian standards and requirements as stated in TEK17. The building was equipped with a radiator, and a hot water tank for domestic hot water supply. The TCCO2HP system was designed to meet the heating demands of the building under various operating conditions. Building characteristics are listed in Table 1 Building design parameters.:

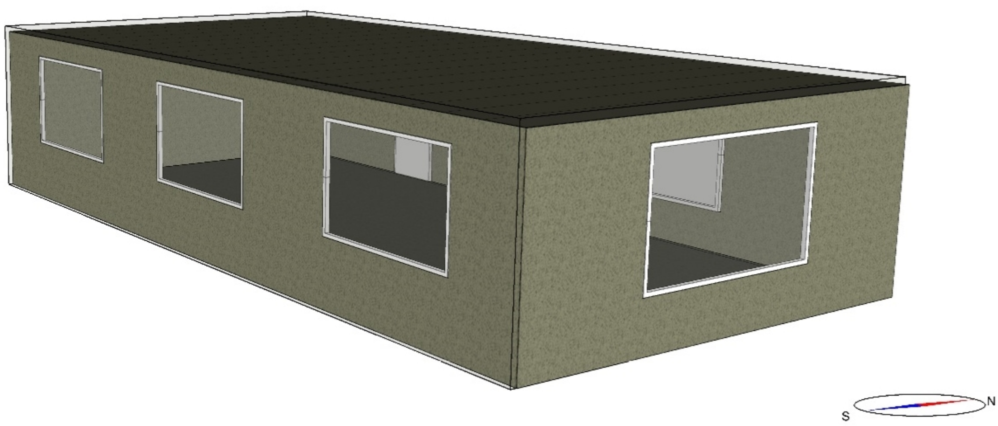

Figure 21 3D layout of the building model in IDA ICE.

Table 1 Building design parameters.

Data category	**Parameter**	**Value**
Areas (m^2)	Floor	75.14
	Walls	74.88
	Roof	75.14
	Windows and door	18.25
U-values ($W/(m^2.K)$)	Internal floor	0.1
	Walls	0.18

	Roof	0.13
	Windows and door	0.8
Material and thickness (m)	Floor	Chip board (0.02), light insulation (0.35), concrete (0.15)
	External walls	Gypsum (0.025), concrete (0.23), light insulation (0.35)
	Internal walls	Gypsum (0.025), light insulation (0.035), Gypsum (0.025)
	Roof	Gypsum (0.02), light insulation (0.4), concrete (0.15), Tar paper (0.005)
Ventilation	Central air handling unit (L/s.m^2)	2
	Thermal bridges (W/(m^2.K))	0.01
	Air change rate at 50 Pa (ACH)	0.5
Internal gains	Equipment	7 units, 160 W/unit
	Lights	5 units, 60 W/unit
	Occupant	3 persons, Activity level 1 MET
Domestic hot water	Average hot water use (L/occ)	50

A typical house living occupancy profile was adopted assumed from IDA ICE database shown in Figure . Lights and equipment were considered having an identical consumption pattern.

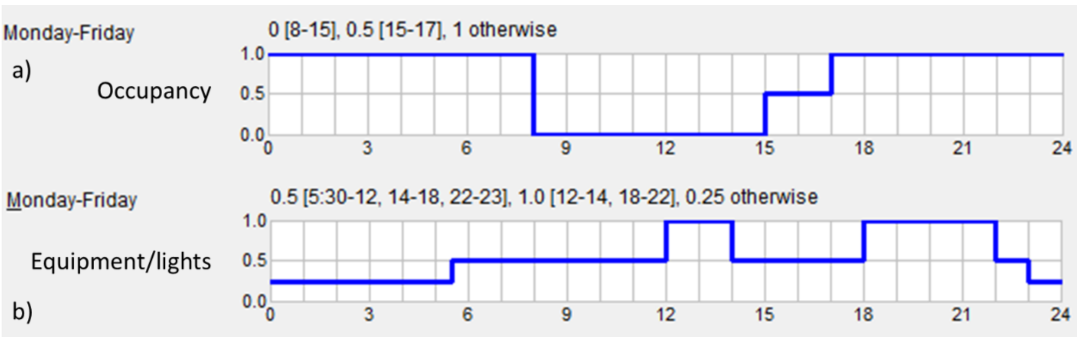

Figure 22 Occupancy gain profiles in the building. a) occupant precences, b) equipment and light consumption intensities.

The sizing process for the described system was done starting from the investigation of the load requirements for the system. The equipment were designed for maximum annual load. This could lead to an oversized system. However, since for the proposed system there are no auxiliary systems provisioned, it was considered that TCCO2HP should be able to cover the entire load. Figure 23 Energy consumption profile of the building in the studied year., shows the annual energy consumption of the building during the design day, as well as temperature variations. Heat demand in the winter peaked up near 3750 W in the winter. Hot water demand was almost 500 W at maximum all year around. The energy profile of the building suggested the need for a maximum 6 kW heat rate capacity on the coldest hour -22°C.

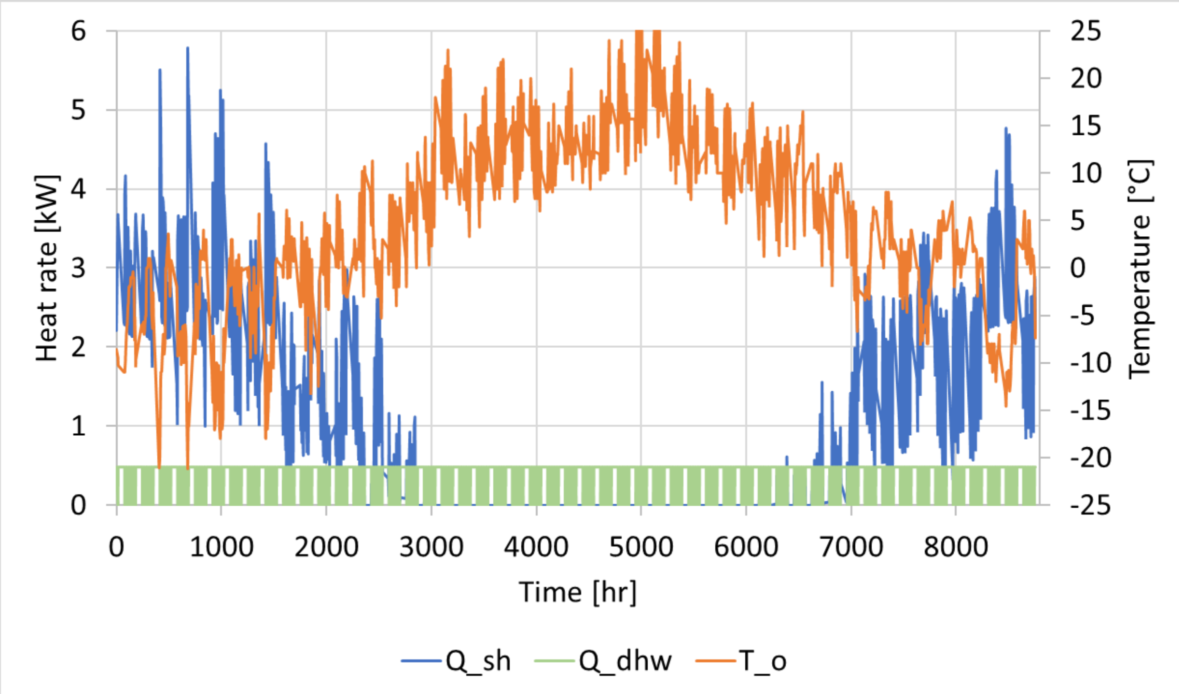

Figure 23 Energy consumption profile of the building in the studied year.

2. Transcritical CO_2 heat pump

The $TCCO_2HP$ components were sized according to the examples of previous studies on similar size of the system. Previous studies have shown high sensitivity of $TCCO_2HP$ operation to design of the system. Meanwhile, designing a tailored $TCCO_2HP$ for a residential application might require a systematic sizing approach as discussed in [72]. Nevertheless, previous studies, in particular, a series of experimental studies in [72, 75] on design and operation of $TCCO_2HP$ by on water-water heating application provided remarkable amount of design configuration data that was used as a guide. In Simscape, the compressor block was parametrized based on the mass flow rate of refrigerant and nominal shaft speed. Other design variables include nominal values of volumetric efficiency, pressure ratio, inlet conditions, mechanical efficiency, and polytropic exponent. In this study a BITZER transcritical compressor with the following specifications was selected. Heat pumps compressor was considered a transcritical 2MTE-4K model manufactured by BITZER company. BITZER provides an online design calculation tool which reports nominal output and input powers, as well as other system parameters such as discharge temperature, mass flow rate for a given pressure range and superheating degree. A similar software called CoolPack was used to analyse the vapour compression cycle of a generic heat pump, where the data from BITZER was used to calculate the missing data such as efficiencies, and rated COP.

The model of the TCCO2HP that described in previous chapters was based on physical relations and interactions of the components. Hence, an accurate model for the working fluid was needed. In this study the CO_2 properties were collected from The National Institute of Standards and Technology (NIST) database. The database included the value of enthalpy, internal energy, enthropy, density, viscousity, thermal conductivity, specific heat capacity. These data were used in a "Two-Phase Fluid Properties (2P)" block in Simscape, used to propagate the CO_2 properties to each calculation point.

3. Water tank sizing

The size of the HWT was determined from the DHW demand of the household. The total hot water consumption was considered 200 L/day. The TES was sized according to the cumulative heat demand curves. As shown in Figure , for most of the year the heat demand was below 60% of the peak load (near 97% of the year). Hence, TES was assumed to have a 40% capacity of peak energy demand (E_{max}). The volume of the TES was calculated as:

$$V_{tes} = \frac{0.4E_{max}}{\rho C_p \Delta T_{max}} \tag{4-1}$$

Where, ΔT_{max} represent the temperature difference of complete discharge. The volume of the tank for the proposed system estimated as 50 litre for a discharge capacity of 2.4 kW.

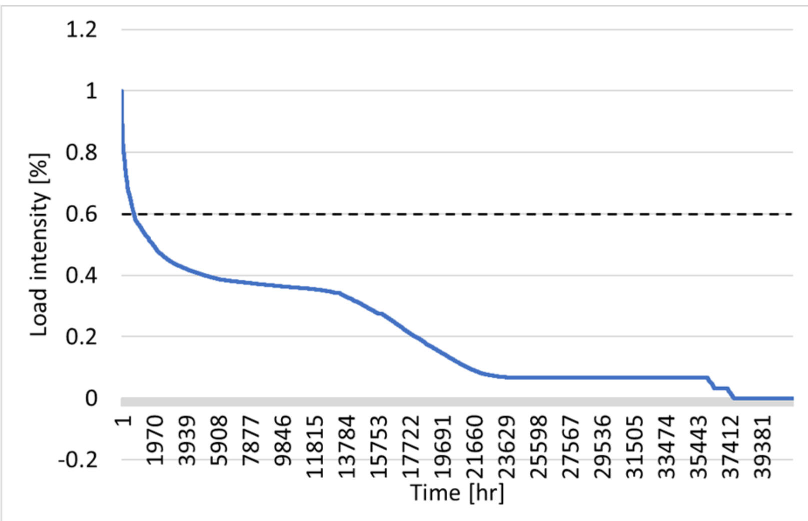

Figure 24 Cumulative curve of energy consumption during a year.

Simulation scenarios

The case study investigated the proposed MPC system in comparison to a conventional controller (CC) scenario . In CC scenario, two proportional controllers were used to maintain the indoor and HWT setpoint temperatures by adjusting the mass flow rates. one PI controller was dedicated to $TCCO_2HP$ expansion valve. The valve controller maintains the compressor discharge pressure. The compressor speed was kept constant.

In MPC scenario, all controllers were replaced by an MPC framework which performed the control actions as explained in previous chapter.

The simulations were performed on 3 example days, namely Winter, Spring, and Summer cases. These cases featured different heat demand profiles. Winter case was characterized by high space heating and DHW demand, as well as generally lower solar gains. Spring day simulated a moderate load on the system, while sudden changes of loads and disturbances were expected. Finally, the summer condition represented a hot water production only situation. In all scenarios the temperature of the surrounding ground was assumed to be constant for the duration of simulations.

5. Results

This chapter presents a evaluation of the residential heating system using ground source $TCCO_2H$. Initially, the focus was on a comparative analysis of the heat pump's operation and the influence of the MPC control approach under various conditions. Subsequently, the chapter delves into a detailed analysis of the data derived from this performance, exploring metrics related to costs, efficiencies, and other pivotal indicators that provide insights into the system's overall effectiveness and efficiency.

The endeavor to implement a linear Model Predictive Control (MPC) model on simplified physical models in MATLAB was fraught with challenges, particularly when aiming for the efficient operation of the MPC controller. A primary concern, which was anticipated, stemmed from the significant divergence of the linear model from the actual nonlinear Simscape system. This divergence is not merely a static issue; it exacerbates as the system's operating point drifts away from its nominal condition.

Drawing from control theory, it's well-understood that linear models are approximations of the real-world systems they represent. While they simplify the complexities for ease of analysis and control, they inherently introduce errors, especially when the system operates in regions far from the point of linearization. This is a fundamental limitation of linear models, and the observed deviation in our study is a manifestation of this inherent challenge.

Given this context, a reactive control scenario emerged as a more fitting choice. The rationale behind this is the relatively lenient demands it places on the dynamic behavior of the system, especially when compared to the MPC. In our study, the conventional control was an ensemble of several Single Input Single Output (SISO) controllers. Each of these controllers was tailored to address a specific control task, allowing for a more compartmentalized and focused approach. This modular nature of SISO controllers can sometimes offer more flexibility in tuning and adapting to specific subsystem behaviors.

Contrastingly, the MPC's approach was holistic. It didn't operate in isolation but took into account all objective functions when determining control moves. While this integrated approach has its merits, especially in systems where interactions between components can't be ignored, it also introduces complexities. In our study, the introduction of multiple constraints, particularly those ensuring the safe operation of the heat pump, further constrained the MPC's decision-making capabilities. The MPC, by design, is a predictive controller that uses a model of the system to predict future outputs and determine control actions that minimize a certain objective function over a prediction horizon. When numerous constraints are added, the optimization problem that the MPC needs to solve becomes more complex and potentially more restrictive.

In comparison, the PI system, with its reactive nature, was less encumbered by these constraints. It responded to errors as they occurred, without the need for predictive modeling and the associated constraints. This made its decisions, in some respects, more flexible than the MPC in our specific application.

In conclusion, while MPC offers a robust and integrated control approach, its efficacy, especially when based on linear models, can be compromised in systems with significant nonlinear behaviors. The choice between MPC and more conventional control strategies, like PID, hinges on the specific requirements and constraints of the system in question. Figures below show the diferrence between the two control technologies in tracking the hot water tank and indoor temperature.

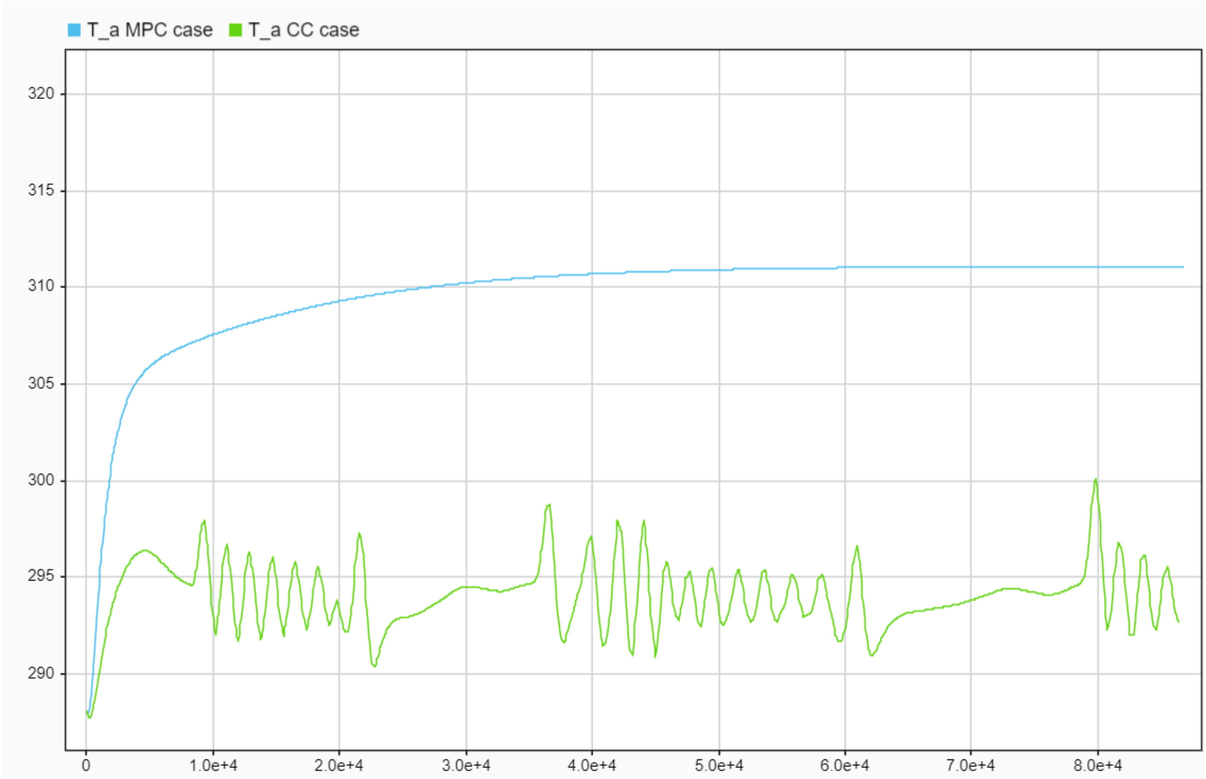

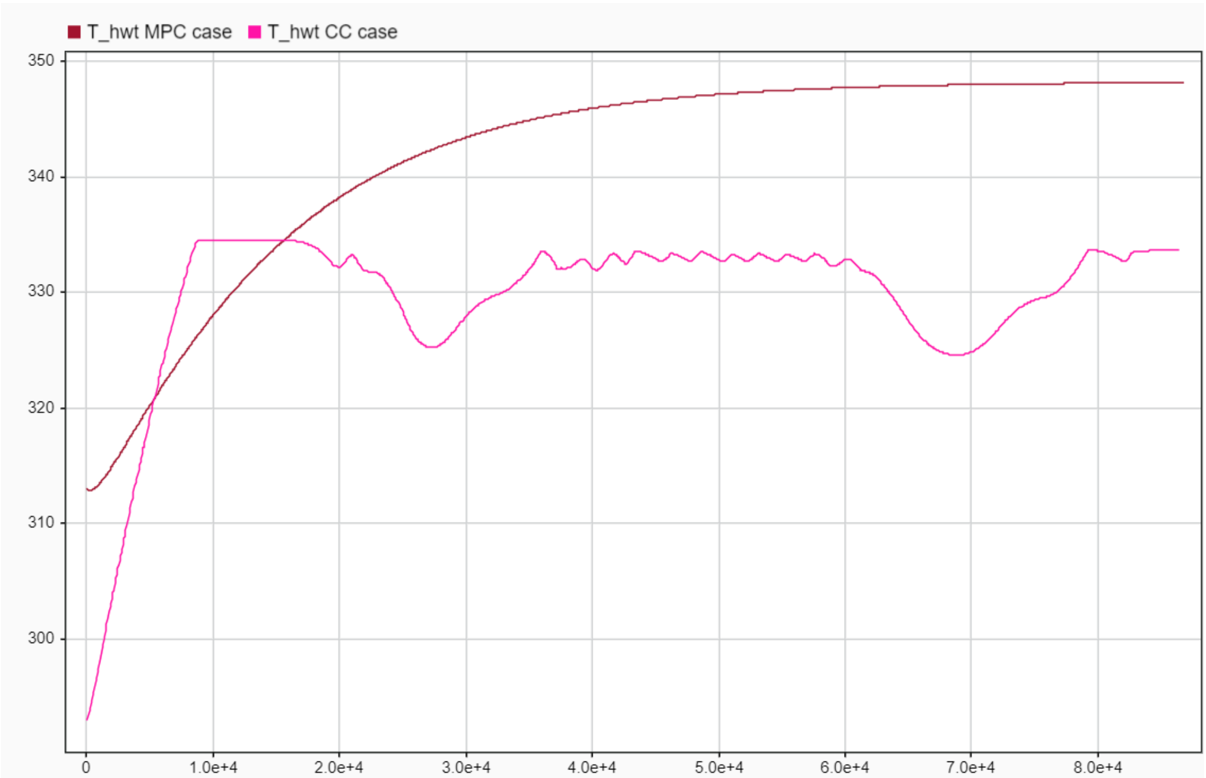

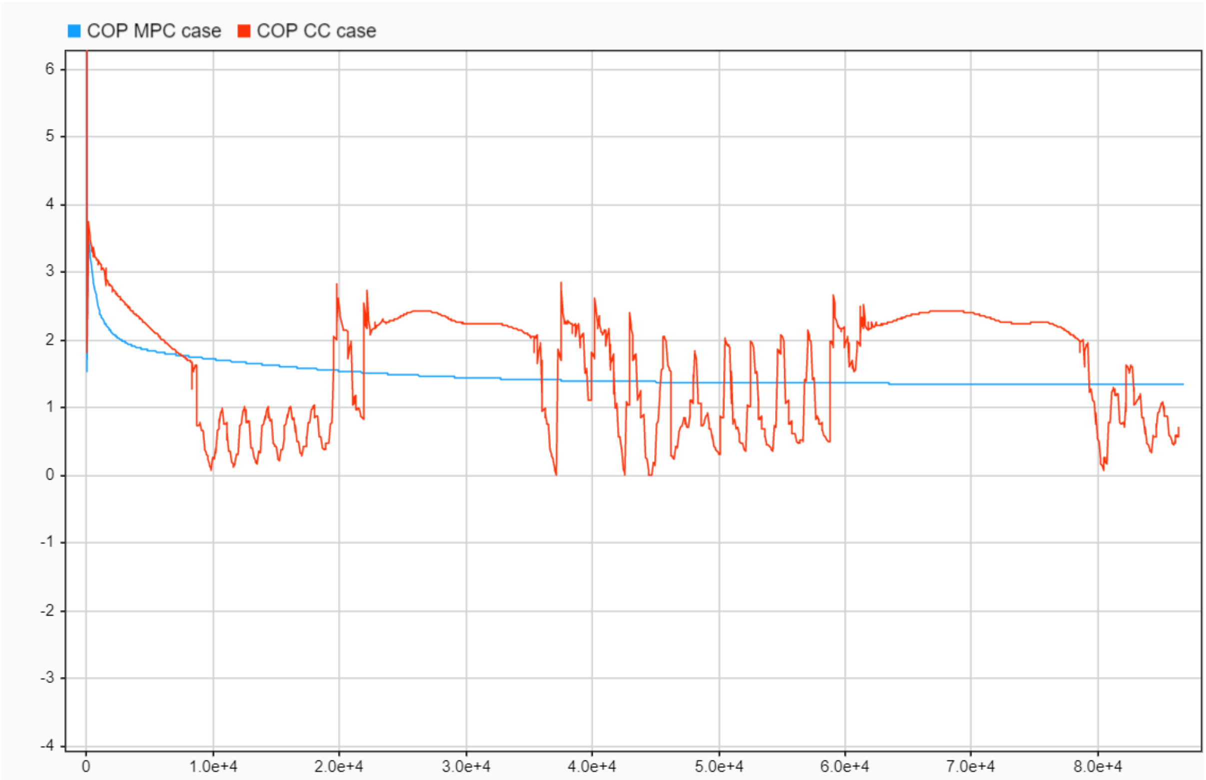

6. Discussion

The realm of control systems has witnessed a plethora of methodologies, each with its unique advantages and challenges. Among these, the Model Predictive Control (MPC) has garnered significant attention due to its predictive nature and ability to handle multi-variable systems. However, the practical implementation of MPC, especially linear versions on platforms like MATLAB, presents its own set of challenges. This chapter delves into the intricacies of such an implementation, juxtaposing it with conventional control strategies.

Linear MPC vs. Nonlinear Realities

At the heart of our discussion is the inherent divergence of a linear MPC model from the actual nonlinear system, as represented in Simscape. Linear models, by design, are approximations tailored for ease of analysis and control. However, they introduce errors, especially when the system operates in regions distant from the point of linearization. As our study revealed, this divergence amplifies as the system's operating point strays from its nominal condition, leading to potential inefficiencies and inaccuracies in control.

The Merits of Reactive Control

Given the challenges with linear MPC, a reactive control scenario, particularly the PID controller, emerged as a more apt choice. The PID controller, being reactive, responds to system errors as they occur, without the complexities of predictive modeling. Its modular nature, especially when implemented as several SISO controllers, offers flexibility in tuning and adapting to specific subsystem behaviors. This compartmentalized approach, where each controller focuses on a specific control task, can sometimes provide more precise control, especially in systems with pronounced nonlinearities.

The Holistic Approach of MPC

Contrary to the modular nature of SISO controllers, MPC adopts a holistic stance. It integrates all objective functions when determining control moves, ensuring a comprehensive control strategy. While this integrated approach is beneficial in systems with significant inter-component interactions, it also introduces complexities. In our study, the addition of multiple constraints, especially those related to the safe operation of the heat pump, made the MPC's decision-making process more intricate and, at times, restrictive.

7. Conclusion

The exploration into the implementation of linear MPC in MATLAB has underscored the nuanced interplay between theoretical control strategies and their practical applications. While MPC offers a promising avenue for integrated and predictive control, its linear incarnation can grapple with challenges, especially when confronted with pronounced nonlinear system behaviors. Reactive control strategies, such as PID, have showcased their resilience and adaptability in certain scenarios, emphasizing that no single control strategy is universally supe Future Research Directions:

Nonlinear MPC Implementation: Given the discrepancies observed with linear MPC, a natural progression would be to delve into nonlinear MPC implementations. This could potentially bridge the gap between the model and the actual system dynamics, enhancing control accuracy.

Hybrid Control Systems: Investigating a hybrid approach, where predictive strategies like MPC are combined with reactive strategies like PID, might yield a system that leverages the strengths of both methodologies.

Adaptive MPC: Research into adaptive MPCs, which can adjust their models in real-time based on system feedback, could provide a dynamic solution to the challenges observed.

Machine Learning and Control: With the advent of AI and machine learning, there's potential to integrate these technologies into control systems. Machine learning algorithms could be employed to refine and adapt control strategies in real-time, enhancing system performance.

Real-world Testing: Beyond simulations in environments like MATLAB, real-world testing of these control strategies on physical systems will provide invaluable insights, helping to bridge the gap between theory and practice.

In essence, the journey into optimizing control strategies is a continuous one, with each study paving the way for more refined and effective solutions.rior.

8. References

1. Hamilton, I., et al., *Global Status Report for Buildings and Construction: Towards a Zero-Emission.* United Nations Environment Programme, Efficient and Resilient Buildings and Construction Sector: Nairobi, Kenya, 2020.
2. Bruno, F., M. Belusko, and E. Halawa, *CO2 refrigeration and heat pump systems—a comprehensive review.* Energies, 2019. **12**(15): p. 2959.
3. Bouckaert, S., et al., *Net Zero by 2050: A Roadmap for the Global Energy Sector.* 2021.
4. Union, E., *Directive (EU) 2018/844 of the European Parliament and of the Council of 30 May 2018 amending Directive 2010/31/EU on the energy performance of buildings and Directive 2012/27/EU on energy efficiency.* Off. J. Eur. Union, 2018. **156**: p. 75-91.
5. Irena, I., *Renewable energy policies in a time of transition: Heating and cooling.* 2020.
6. Calise, F., et al., *Dynamic modelling and thermoeconomic analysis for the energy refurbishment of the Italian building sector: case study for the "Superbonus 110%" funding strategy.* Applied Thermal Engineering, 2022: p. 118689.
7. López Paniagua, I., et al., *Comparison of transcritical CO2 and conventional refrigerant heat pump water heaters for domestic applications.* Energies, 2019. **12**(3): p. 479.
8. Willem, H., Y. Lin, and A. Lekov, *Review of energy efficiency and system performance of residential heat pump water heaters.* Energy and Buildings, 2017. **143**: p. 191-201.
9. Nair, V., *HFO refrigerants: A review of present status and future prospects.* International Journal of Refrigeration, 2021. **122**: p. 156-170.
10. Schulz, M. and D. Kourkoulas, *Regulation (EU) No 517/2014 of The European Parliament and of the council of 16 April 2014 on fluorinated greenhouse gases and repealing Regulation (EC) No 842/2006.* Off. J. Eur. Union, 2014. **2014**(517): p. L150.

11. Velders, G.J., et al., *The importance of the Montreal Protocol in protecting climate.* Proceedings of the National Academy of Sciences, 2007. **104**(12): p. 4814-4819.
12. Khanam, M. and T.U. Daim, *A regional technology roadmap to enable the adoption of CO2 heat pump water heater: A case from the Pacific Northwest, USA.* Energy Strategy Reviews, 2017. **18**: p. 157-174.
13. Abas, N., et al., *Natural and synthetic refrigerants, global warming: A review.* Renewable and Sustainable Energy Reviews, 2018. **90**: p. 557-569.
14. Song, Y., et al., *Advanced development and application of transcritical CO2 refrigeration and heat pump technology—A review.* Energy Reports, 2022. **8**: p. 7840-7869.
15. Wang, S., et al., *Experimental investigation on air-source transcritical CO2 heat pump water heater system at a fixed water inlet temperature.* International Journal of Refrigeration, 2013. **36**(3): p. 701-716.
16. Qi, P.-C., et al., *Experimental investigation of the optimal heat rejection pressure for a transcritical CO2 heat pump water heater.* Applied Thermal Engineering, 2013. **56**(1-2): p. 120-125.
17. Cao, F., Z. Ye, and Y. Wang, *Experimental investigation on the influence of internal heat exchanger in a transcritical CO2 heat pump water heater.* Applied Thermal Engineering, 2020. **168**: p. 114855.
18. Liu, X., et al., *Energetic, environmental and economic comparative analyses of modified transcritical CO2 heat pump system to replace R134a system for home heating.* Energy, 2021. **229**: p. 120544.
19. Kim, M.-H., J. Pettersen, and C.W. Bullard, *Fundamental process and system design issues in CO2 vapor compression systems.* Progress in energy and combustion science, 2004. **30**(2): p. 119-174.
20. Peng, X., et al., *Experimental investigation and comparison on heating performance characteristics of two transcritical CO2 heat pump systems.* Energy and Buildings, 2021. **250**: p. 111296.
21. Hu, B., et al., *Extremum seeking control of COP optimization for air-source transcritical CO2 heat pump water heater system.* Applied Energy, 2015. **147**: p. 361-372.
22. Otón-Martínez, R.A., et al., *Impact of an internal heat exchanger on a transcritical CO2 heat pump under optimal pressure conditions: Optimal-pressure performance of CO2 heat pump with IHX.* Applied Thermal Engineering, 2022. **215**: p. 118991.
23. Yang, L., et al., *Analysis and comparison of influence factors of hot water temperature in transcritical CO2 heat pump water heater: An experimental study.* Energy Conversion and Management, 2019. **198**: p. 111836.
24. Illán-Gómez, F., et al., *Evaluation of the Use of Different Dedicated Mechanical Subcooling (DMS) Strategies in a Water Source Transcritical CO2 Heat Pump for Space Heating Applications.* Clean Technologies, 2022. **4**(4): p. 1208-1226.
25. Zhang, Z., et al., *Influence of refrigerant charge amount and EEV opening on the performance of a transcritical CO2 heat pump water heater.* Energies, 2017. **10**(10): p. 1521.
26. Illán-Gómez, F., et al., *Numerical performance of a water source transcritical CO2 heat pump with mechanical subcooling.* Applied Thermal Engineering, 2023. **219**: p. 119639.
27. LI, Y., et al., *Effect of electronic expansion valve opening on discharge pressure of a water-source CO2 heat pump: An experimental study.*
28. Li, Y., et al. *Study of a water-source CO2 heat pump for residential use: experimental discharge pressure control and performance analysis*. in *E3S Web of Conferences*. 2021. EDP Sciences.
29. Cui, C., et al., *Multi-variable extreme seeking control for efficient operation of sub-cooler vapor injection trans-critical CO2 heat pump water heater.* Applied Thermal Engineering, 2021. **184**: p. 116261.
30. Bastani, A., et al., *Experimental characterization of a transcritical CO2 direct expansion ground source heat pump for heating applications.* Energy and Buildings, 2020. **212**: p. 109828.

31. Wu, W., H.M. Skye, and J.J. Dyreby, *Modeling and experiments for a CO2 ground-source heat pump with subcritical and transcritical operation.* Energy Conversion and Management, 2021. **243**: p. 114420.
32. Drgoňa, J., et al., *All you need to know about model predictive control for buildings.* Annual Reviews in Control, 2020. **50**: p. 190-232.
33. Afroz, Z., et al., *Modeling techniques used in building HVAC control systems: A review.* Renewable and sustainable energy reviews, 2018. **83**: p. 64-84.
34. Taheri, S., P. Hosseini, and A. Razban, *Model predictive control of heating, ventilation, and air conditioning (HVAC) systems: A state-of-the-art review.* Journal of Building Engineering, 2022: p. 105067.
35. Seborg, D.E., et al., *Process dynamics and control*. 2016: John Wiley & Sons.
36. Mariano-Hernández, D., et al., *A review of strategies for building energy management system: Model predictive control, demand side management, optimization, and fault detect & diagnosis.* Journal of Building Engineering, 2021. **33**: p. 101692.
37. Stadler, P., et al., *Contribution of model predictive control in the integration of renewable energy sources within the built environment.* Frontiers in Energy Research, 2018. **6**: p. 22.
38. Yang, S., et al., *An adaptive robust model predictive control for indoor climate optimization and uncertainties handling in buildings.* Building and Environment, 2019. **163**: p. 106326.
39. Hou, J., et al., *Model predictive control under weather forecast uncertainty for HVAC systems in university buildings.* Energy and Buildings, 2022. **257**: p. 111793.
40. Raman, N.S., B. Chen, and P. Barooah, *On energy-efficient HVAC operation with Model Predictive Control: A multiple climate zone study.* Applied Energy, 2022. **324**: p. 119752.
41. Austin, B.T. and K. Sumathy, *Transcritical carbon dioxide heat pump systems: A review.* Renewable and Sustainable Energy Reviews, 2011. **15**(8): p. 4013-4029.
42. Ramazanova, A.E. and I.M. Abdulagatov, *Thermal Conductivity of Supercritical CO2-Saturated Coal.* International Journal of Thermophysics, 2020. **42**(1): p. 2.
43. Nekså, P., et al., *CO2-heat pump water heater: characteristics, system design and experimental results.* International Journal of Refrigeration, 1998. **21**(3): p. 172-179.
44. Lo Basso, G., et al., *The potential role of trans-critical CO2 heat pumps within a solar cooling system for building services: The hybridised system energy analysis by a dynamic simulation model.* Renewable Energy, 2021. **164**: p. 472-490.
45. Maddah, S. and M.R. Safaei, *Determination of the optimal discharge pressure of the transcritical CO2 heat pump cycles for heating and cooling performances based on new correlation.* Journal of Thermal Analysis and Calorimetry, 2021. **145**(3): p. 1537-1546.
46. Nekså, P., *CO2 heat pump systems.* International Journal of Refrigeration, 2002. **25**(4): p. 421-427.
47. Illán-Gómez, F., et al., *Experimental and numerical study of a CO2 water-to-water heat pump for hot water generation.* International Journal of Refrigeration, 2021. **132**: p. 30-44.
48. Liu, X., et al., *Experimental study on the performance of water source trans-critical CO2 heat pump water heater.* Energies, 2017. **10**(6): p. 810.
49. Schiefloe, P. and P. Nekså, *CO2 varmepumpe for bygningsoppvarming, forprosjekt.* SINTEF Report. Trondheim, SINTEF Energy Research, 1999.
50. Foulds, E., M. Abeysekera, and J. Wu, *Modelling and analysis of a ground source heat pump combined with a PV-T and earth energy storage system.* Energy Procedia, 2017. **142**: p. 886-891.
51. Zhang, C., et al., *Thermal behavior of a combi-storage in a solar-ground source heat pump system for a single-family house.* Energy and Buildings, 2022. **259**: p. 111902.
52. Rieberer, R., G. Kasper, and H. Halozan, *CO2. A chance for once-through heat pump heaters.* 1998.
53. Rieberer, R., et al., *CO2 heat pumps in controlled ventilation systems. Discussion.* Science et technique du froid, 1998: p. 212-222.

54. Stene, J., *Residential CO2 heat pump system for combined space heating and hot water heating.* International Journal of Refrigeration, 2005. **28**(8): p. 1259-1265.
55. Wang, Z., et al., *Experimental investigation on thermal characteristics of transcritical CO2 heat pump unit combined with thermal energy storage for residential heating.* Applied Thermal Engineering, 2020. **165**: p. 114505.
56. Wang, Z., et al., *Investigation on the feasibility and performance of transcritical CO2 heat pump integrated with thermal energy storage for space heating.* Renewable Energy, 2019. **134**: p. 496-508.
57. Wang, W., et al., *Model predictive control for the operation of a transcritical CO2 air source heat pump water heater.* Applied Energy, 2021. **300**: p. 117339.
58. Brodal, E. and S. Jackson, *A comparative study of CO2 heat pump performance for combined space and hot water heating.* International Journal of Refrigeration, 2019. **108**: p. 234-245.
59. Verhelst, C., et al., *Study of the optimal control problem formulation for modulating air-to-water heat pumps connected to a residential floor heating system.* Energy and Buildings, 2012. **45**: p. 43-53.
60. Oviedo-Cepeda, J.C., F.Z. Amara, and A.K. Athienitis. *Model Predictive Control Horizon Impact over the Flexibility of a Net Zero Energy Building*. in *IECON Proceedings (Industrial Electronics Conference)*. 2021.
61. Bianco, G., et al., *A hierarchical Building Management System for temperature?s optimal control and electric vehicles? integration.* ENERGY CONVERSION AND MANAGEMENT-X, 2023. **17**.
62. Chen, W.H. and F. You, *Building Climate Control with Hybrid Renewable Energy Systems Using Data-Driven Robust Model Predictive Control.* Chemical Engineering Transactions, 2022. **94**: p. 499-504.
63. Chen, W.H. and F. You, *Sustainable building climate control with renewable energy sources using nonlinear model predictive control.* Renewable and Sustainable Energy Reviews, 2022. **168**.
64. Chen, Y., et al. *A Model-Based Predictive Control Method of the Ground-Source Heat Pump System for Maintaining Thermal Comfort in Low-Energy Buildings*. in *2022 IEEE 7th International Conference on Power and Renewable Energy, ICPRE 2022*. 2022.
65. Fitó, J., et al., *Robustness of district heating versus electricity-driven energy system at district level: A multi-objective optimization study.* Smart Energy, 2022. **6**.
66. Toradmal, A., T. Kemmler, and B. Thomas, *Boosting the share of onsite PV-electricity utilization by optimized scheduling of a heat pump using buildings thermal inertia.* APPLIED THERMAL ENGINEERING, 2018. **137**: p. 248-258.
67. Jeon, B.-K. and E.-J. Kim, *White-Model Predictive Control for Balancing Energy Savings and Thermal Comfort.* Energies, 2022. **15**(7): p. 2345.
68. Chen, W.H. and F. You, *An Energy Optimization Model for Commercial Buildings with Renewable Energy Systems via Nonlinear MPC.* Chemical Engineering Transactions, 2022. **94**: p. 505-510.
69. Chen, W.H. and F.Q. You, *Sustainable building climate control with renewable energy sources using nonlinear model predictive control.* RENEWABLE & SUSTAINABLE ENERGY REVIEWS, 2022. **168**.
70. Zhang, T., et al., *The model predictive control strategy of the transcritical CO2 air conditioning system used in railway vehicles.* Applied Thermal Engineering, 2023. **218**: p. 119376.
71. Coder, H., *MathWorks.* Inc. URL: https://www. mathworks. com/help/ecoder/index. html, 2016.
72. Li, Y., et al., *Model-based sizing of a CO2 heat pump for residential use.* Sustainable Energy Technologies and Assessments, 2022. **53**: p. 102592.

73. Agrawal, N. and S. Bhattacharyya, *Optimized transcritical CO2 heat pumps: Performance comparison of capillary tubes against expansion valves.* International Journal of Refrigeration, 2008. **31**(3): p. 388-395.
74. Urresta, E., et al., *Ground thermal conductivity estimation using the thermal response test with a horizontal ground heat exchanger.* Geothermics, 2021. **96**: p. 102213.
75. Li, Y. and N. Nord. *Performance analysis of water-to-water CO2 heat pump in different compressor rotational speed*. in *CLIMA 2022 conference*. 2022.

9.